

©2019

Chan Yang

ALL RIGHTS RESERVED

ANALYSIS OF STEEL TRUSS BRIDGES WITHOUT PLANS

by

CHAN YANG

A thesis submitted to the

School of Graduate Studies

Rutgers, The State University of New Jersey

in partial fulfillment of the requirements

for the degree of

Master of Science

Graduate Program in Civil and Environmental Engineering

written under the direction of

Dr. Hani H. Nassif

and approved by

New Brunswick, New Jersey

May 2019

ABSTRACT OF THE THESIS

ANALYSIS OF STEEL TRUSS BRIDGES WITHOUT PLANS

By CHAN YANG

Thesis Director:

Dr. Hani H. Nassif

The bridge load rating provides a basis for determining the safe load carrying capacity of a bridge to ensure the bridge serviceability and safety. In New Jersey, a large number of steel truss bridges, including historical bridges, are currently in service. In the case that the as-built plans of a bridge are missing or not available, a particular challenge is raised for the agencies and engineers to determine the capacity of the structural members. Relying on the engineering judgement alone may lead to an inefficient load posting. Thus, a reliable methodology, which could also reduce the amount of work needed for the agencies to do the field investigations, is needed to load rate the steel truss bridges with no plans.

The proposed load rating procedure involves using the clustering methodology. The clustering methodology estimates the member sizes based on the similar bridges which were built in the same decade and have the same structural type, as well as similar geometries. This thesis focuses on finding the correlations between the member sizes and bridge geometries. The information of six (6) bridges from NJDOT bridge inventory were analyzed to construct the parametric study. From the study, it is found that the member sizes have strong correlations with geometries, such as stringer spacing, floorbeam length,

bridge width, etc. The unknown member sizes then estimated based on the bridges with plans that have similar bridge geometries. The estimation results are then validated by the field inspection, proving the effectiveness of the clustering methodology. The accuracy of the clustering approach can be further improved by incorporating more bridges with plans into the cluster.

The load rating of one bridge without plans is performed in this study. In order to refine the rating factors, the Finite Element Model (FEM) and the advanced technology of Weight-in-Motion (WIM) system were also applied in this thesis. It is found that the FEM can significantly reduce the live load effects on the floorbeam compared with the line girder analysis using American Association of State Highway and Transportation Officials (AASHTO) LRFD Specification Girder Distribution Factor (GDF) equation. Furthermore, the WIM data was applied to find site-specific live load factor in order to better address the live load uncertainties within the specific region. The final load rating results indicate that there is no need to post load limitation for the target bridge without plans.

ACKNOWLEDGMENTS

I would like to thank my advisor, Dr. Hani Nassif, for his continuous support throughout my study at Rutgers. It has been a great honor for me to have him as my advisor, who is always there giving me guidance, encouragement, and knowledge.

I would like to thank Dr. Yook-Kong Yong and Dr. Peng Lou for being on my thesis committee and their valuable advice.

I would like to thank Dr. Peng Lou for being a wonderful mentor for me and helping me to get started with this research

I would like to thank my work colleagues, graduate assistant, Dongjian Gao, He Zhang, post-doctoral associate Dr. Graziano Fiorillo, research associate Dr. Adi Abu-Obeidah and Dr. Chaekuk Na for their helpful suggestion, fruitful discussion and also being my friends. Their experiences in life and engineering field help me get through all the obstacles during my work. They create a harmonious atmosphere with fun for the people working here.

I would like to thank my father and mother who always give me unconditionally love, cares and supports. They help me grow and shape me into the person I am today. I would like to thank my friend Bingqing Xiang for always providing support.

TABLE OF CONTENTS

ABSTRACT OF THE THESIS	ii
ACKNOWLEDGMENTS	iv
TABLE OF CONTENTS.....	v
LIST OF TABLES	viii
LIST OF FIGURES	xi
1. Introduction.....	1
1.1. Background	1
1.2. Objectives	2
2. Literature Review.....	4
2.1. General Load Rating Procedures using Load and Resistance Factor Rating (LRFR)	4
2.2. General Studies on Load Rating for Steel Truss Bridge without Plans	7
2.3. Load Rating Using Site-Specific Weigh-in-Motion (WIM) Data	8
3. Analysis of Bridges without Plans Using Bridge Clustering Methodology	14
3.1. Clustering Methodology.....	14
3.1.1. Critical Parameters Related to Load Rating of Steel Truss Bridges	14
3.1.2. Development of Bridge Clustering Methodology.....	15
3.2. Analysis of Structural Element Capacity with Respect to Bridge Dimensions .	18
3.2.1. Stringer	19

3.2.2.	Floorbeam	20
3.2.3.	Truss Member	22
3.3.	Obtaining the Member Sizes of the Bridge without Plans	26
3.3.1.	Estimation of the Member Size Using Clustering Method	26
3.3.2.	Validation of the Clustering Results by Field Inspection	30
4.	Load Rating of the Bridge with No Plans	34
4.1.	Proposed Procedures for Load Rating the Steel Truss Bridge with No Plans ...	34
4.2.	Analysis of Member Capacity	35
4.2.1.	Stringer Resistance.....	35
4.2.2.	Floorbeam Resistance	38
4.2.3.	Truss Member Resistance	39
4.3.	Live Load Effects using AASHTO GDF Equations	42
4.4.	Live Load Effects Using Finite Element Model	45
5.	Analysis of Site-Specific Live Load Factor of Legal Load	49
5.1.	Generalized Live Load Factors, γ_L for Routine Commercial Traffic.....	49
5.2.	Site- Specific Live Load Factors	50
5.2.1.	Introduction and Motivation	50
5.2.2.	General Expressions for Site-Specific Live Load Factors	52
5.3.	Estimation of the Maximum Load Effect, L_{max}	56
5.3.1.	Gumbel Distribution	57

5.3.2.	Normal Distribution	59
5.4.	WIM Data Processing Demonstration.....	61
5.4.1.	Step One: Read Data	61
5.4.2.	Step Two: Hypothesis Testing	61
5.4.3.	Step Three: Estimation of L_{\max} and γ_L	62
5.5.	Proposed Live Load Factor for the Bridge with No Plan.....	68
6.	Load Rating Results	70
6.1.	Load Rating Results using Clustering Methodology	70
6.2.	Load Rating Results using Field Investigation	72
6.3.	Refinement of the Design Load Rating Using FEM	74
6.4.	Legal Load Rating Using Site-Specific Live Load Factor	75
7.	Conclusions.....	78
	REFERENCES	82

LIST OF TABLES

Table 1 – Unknown Parameters of Steel Bridge with No Plans	15
Table 2 – Steel Truss Floorbeam System Bridges with Plans	18
Table 3 – Summary of the Correlative Factors	27
Table 4 – Summary of the Stinger Sections.....	28
Table 5 – Summary of the Floorbeam Sections.....	28
Table 6 – Summary of the Truss Member Sections.....	30
Table 7 – Comparison between Field Inspection and Clustering Method.....	33
Table 8 – Calculation of \bar{Y} and M_p for Sections in Positive Flexure	36
Table 9 – Plate Buckling Coefficients and Width of Plates for Axial Compression (AASHTO LRFD, 2017)	40
Table 10 – Distribution of Live Loads for Moment in Interior Beam	43
Table 11 – Distribution of Live Loads for Shear in Interior Longitudinal Beam.....	43
Table 12 – Distribution of Live Loads for Moment in Exterior Longitudinal Beam	43
Table 13 – Distribution of Live Loads for Shear in Exterior Longitudinal Beam.....	44
Table 14 – Summary of Girder Distribution Factors for Structure No. 020033G.....	44
Table 15 – Hand Calculation Results- Live Load Effects on the Floorbeam	48
Table 16 – Finite Element Model Outputs- Live Load Effects on the Floorbeam	48
Table 17 – Generalized Live Load Factors, γ_L for Routine Commercial Traffic	50
Table 18 – WIM Site for Developing the Site-Specific Live Load Factors	52
Table 19 - Mean Maximum Moments for Simple Spans Decided by Corresponding New LRFD Moment (Nowak, 1999).....	53

Table 20 – Comparisons of the Simulated Mean Maximum Lane Moment, HL93, AASHTO Legal Vehicles and HS20 Load Models (Moses, 2001)	54
Table 21 – Bias Ratio for Simple Span (WIM Site CO082116).....	66
Table 22 – Percent Difference of Gumbel Distribution vs. Normal Distribution – Positive Moment	67
Table 23– Percent Difference of Gumbel Distribution vs. Normal Distribution – Negative Moment	68
Table 24 – Proposed Site-Specific Live Load Factor, γ_L	69
Table 25 - Interior Stringer Rating Factors Based on Clustering Methodology	70
Table 26 - Exterior Stringer Rating Factors Based on Clustering Methodology.....	70
Table 27 - Floorbeam Rating Factors Based on Clustering Methodology	71
Table 28 – Top Chord Rating Factors Based on Clustering Methodology.....	71
Table 29 – Bottom Chord Rating Factors Based on Clustering Methodology	71
Table 30 – Diagonal Rating Factors Based on Clustering Methodology	71
Table 31 - Interior Stringer Rating Factors Based on Field Inspection	72
Table 32 - Exterior Stringer Rating Factors Based on Field Inspection	72
Table 33 – Floorbeam Rating Factors Based on Field Inspection	73
Table 34 – Top Chord Rating Factors Based on Field Inspection	73
Table 35 – Bottom Chord Rating Factors Based on Field Inspection	73
Table 36 – Diagonal Rating Factors Based on Field Inspection.....	73
Table 37 – Refined Rating Factors of Floorbeam Using Finite Element Model	75
Table 38 – Refined Interior Stringer Rating Factors for Legal Loads	76
Table 39 – Refined Exterior Stringer Rating Factors for Legal Loads.....	76

Table 40 – Refined Floorbeam Rating Factors for Legal Loads	76
Table 41 – Refined Top Chord Rating Factors for Legal Loads	77
Table 42 – Refined Bottom Chord Rating Factors for Legal Loads.....	77
Table 43 – Refined Diagonal Rating Factors for Legal Loads	77

LIST OF FIGURES

Figure 1. Load and Resistance Factor Rating Flow Chart (AASHTO MBE 3 nd Edition) ..	6
Figure 2. Typical Appearance of the Pony Truss	17
Figure 3. Stringer Capacity vs. Stringer Length for Steel Truss Bridge	20
Figure 4. Stringer Capacity vs. Stringer Spacing for Steel Truss Bridge	20
Figure 5. Stringer Capacity vs. Floorbeam Length for Steel Truss Bridge	22
Figure 6. Stringer Capacity vs. Floorbeam Spacing for Steel Truss Bridge	22
Figure 7. Configuration of the Typical Steel Truss Through Bridge.....	23
Figure 8. Truss Member Cross-Sectional Area vs. Distance between Truss Centerlines.	25
Figure 9. Truss Member Cross-Sectional Area vs. Member Length	26
Figure 10. Truss Member Cross-Sectional Area vs. Bridge Span Length.....	26
Figure 11. Overview of Structure No. 020033G.....	31
Figure 12. Field Inspection on structure No. 030033G	32
Figure 13. Guideline for Load Rating the Steel Truss Bridges without Plans.....	34
Figure 14. Dead Load Effects of the Bridge with No Plan (SN. 020033G)	41
Figure 15. Cross-Section View of the Truss Bridge & Schematic Drawing of the Live Load Applied to the Floorbeam Based on Hand Calculation	46
Figure 16. Abaqus Model for the Bridge with No Plans (SN. 020033G).....	47
Figure 17. Demonstration of Estimating L_{max} assuming Gumbel Distribution	62
Figure 18. Demonstration of Estimating L_{max} assuming Normal Distribution	64

Chapter I

1. Introduction

1.1. Background

In New Jersey, a large number of steel bridges, including steel truss bridges, are in service in either highway or local areas. The bridge service life is sometimes found to be much shorter than it was designed for due to the unexpected deterioration or structure's fracture. The periodic inspection and bridge evaluation can help to investigate the level of structural safety. In order to optimize the economic value and ensure public safety, the New Jersey Department of Transportation (NJDOT) instituted the mandated bridge safety inspection program starting in 1971. Bridge load rating provides a basis for determining the safe load capacity of a bridge. The premise of performing bridge load rating is that sufficient information about the structural element are available so that the member resistance can be determined. For the bridges with plans, the rating factors can be easily determined based on the known parameters. However, there exists the case that the bridge plans were missing due to either the old age of the bridge or the improper storage of the owner, especially for the historic bridges or the private-owned bridges. NJDOT has also recognized some steel bridges that are missing the original plans, among which the steel truss bridges built in the 1990s are the majority. These bridges are mostly located in rural areas instead of on the highway.

To begin the research on how to evaluate the bridges with no plans, inspection reports, which usually includes the rating factors, were obtained from NJDOT. It is observed that

if the structures are in good conditions based on the periodic inspection, the rating factors are directly determined by engineering judgment without any investigation on the load effects and the structural resistance. Based on the literature from other agencies, engineering judgment is also widely used to load rate the bridges with no plans. However, engineering judgment tends to be overly conservative, leading to unnecessary load postings and traffic restrictions. As a result, a more scientific and reliable load rating methodology for the steel truss bridges with no plans, which can reflect the actual bridge load carrying capacity, is needed.

Besides the deterioration caused by the corrosive environment, human factors are also leading factors that reduces the service life of a bridge, such as the high traffic flow and overweight truck traffic. The live load, as reflected by the live load factor that is higher than any other load factors, include many of the uncertainties. The loading conditions, like ADTT and truck weights, are expected to be very different for different road classes so that the traffic conditions can vary drastically from site to site. In order to conduct more accurate bridge ratings, site-to-site variability of live loads should be taken into considerations.

1.2. Objectives

Bridges without plans create a particular challenge to the agencies when the bridges are in need of load rating. From the literature review, it was found that other state agencies or DOTs do not have explicit solutions towards this problem. The main objective of this research is to propose a scientific load rating methodology for the steel truss bridges with no plans by incorporating with Load and Resistance Factor Rating (LRFR). As will be

discussed later in this paper, a clustering methodology which involves using the correlations between the similar bridges is proposed to estimate the unknown member sizes. The clustering method is applied to one bridge without plans in this study. For the purpose of both validating the clustering methodology and improving the accuracy of the rating factors, the actual bridge dimensions and member sizes also measured in the sites.

Furthermore, the finite element model (FEM) is utilized in this study to investigate accurate live load effects. Current AASHTO LRFD presents the equations for calculating girder distribution factors (GDF) to determine how many live loads each girder resists; however, the stringers usually do not all into the applicable ranges of these equations. In addition, the live load effects are found to be overly estimated by using the line girder analysis. In this case, the finite element models are required to determine the actual live load effects.

In addition, Weigh-in-Motion (WIM) technology are also involved in order to improve the accuracy of the rating factors. The AASHTO MBE has presented the generalized live load factors. However, the live load can vary hugely for the different road classes. In this study, the site-specific live load factors will be determined for the bridge based on the data collected from six (6) WIM stations that locate in the same county where the bridge located at.

Chapter II

2. Literature Review

2.1. General Load Rating Procedures using Load and Resistance Factor Rating (LRFR)

- 2018- American Association of State Highway and Transportation Officials
Manual for Bridge Evaluation, 3rd ed.

The American Association of State Highway and Transportation Officials (AASHTO) Manual for Bridge Evaluation (MBE) is to serve as a resource for use in developing specific policy and procedures for the inspection and evaluation of existing in-service bridges. MBE required collecting the comprehensive bridge data before load rating a bridge, including the geometric data, member and condition data, and the loading and traffic data. The geometric data can be collected by the drawings easily, but the condition data and traffic data will need to be obtained thoroughly by field investigation. The general load-rating factor is calculated by Equation (1):

$$RF = \frac{C - \gamma_{DC}(DC) - \gamma_{DW}(DW) \pm \gamma_P(P)}{\gamma_{LL}(LL + IM)} \quad (1)$$

where

C = capacity

DC = dead load effect due to structural components and attachments

DW = dead load effect due to wearing surface and utilities

P = permanent loads other than dead loads

LL = live load effect

γ_{DC} = LRFD load factor for structural components and attachments

γ_{DW} = LRFD load factor for wearing surfaces and utilities

γ_P = LRFD load factor for permanent loads other than dead loads = 1.0

γ_{LL} = evaluation live load factor

Among these factors, capacity C is related to the structure conditions. If damages or deteriorations are inspected, capacity reduction might be necessary to be considered. The dead load effects can be straightforwardly calculated as long as all the geometric data are known. Regarding the live load effects, there are three levels of load-rating to be performed in LRFR: 1) design-load rating, 2) legal-load rating, and 3) permit-load rating. Each level indicates different specific live load targets. The procedure Load and Resistance Factor Rating Flow Chart is shown in Figure 1.

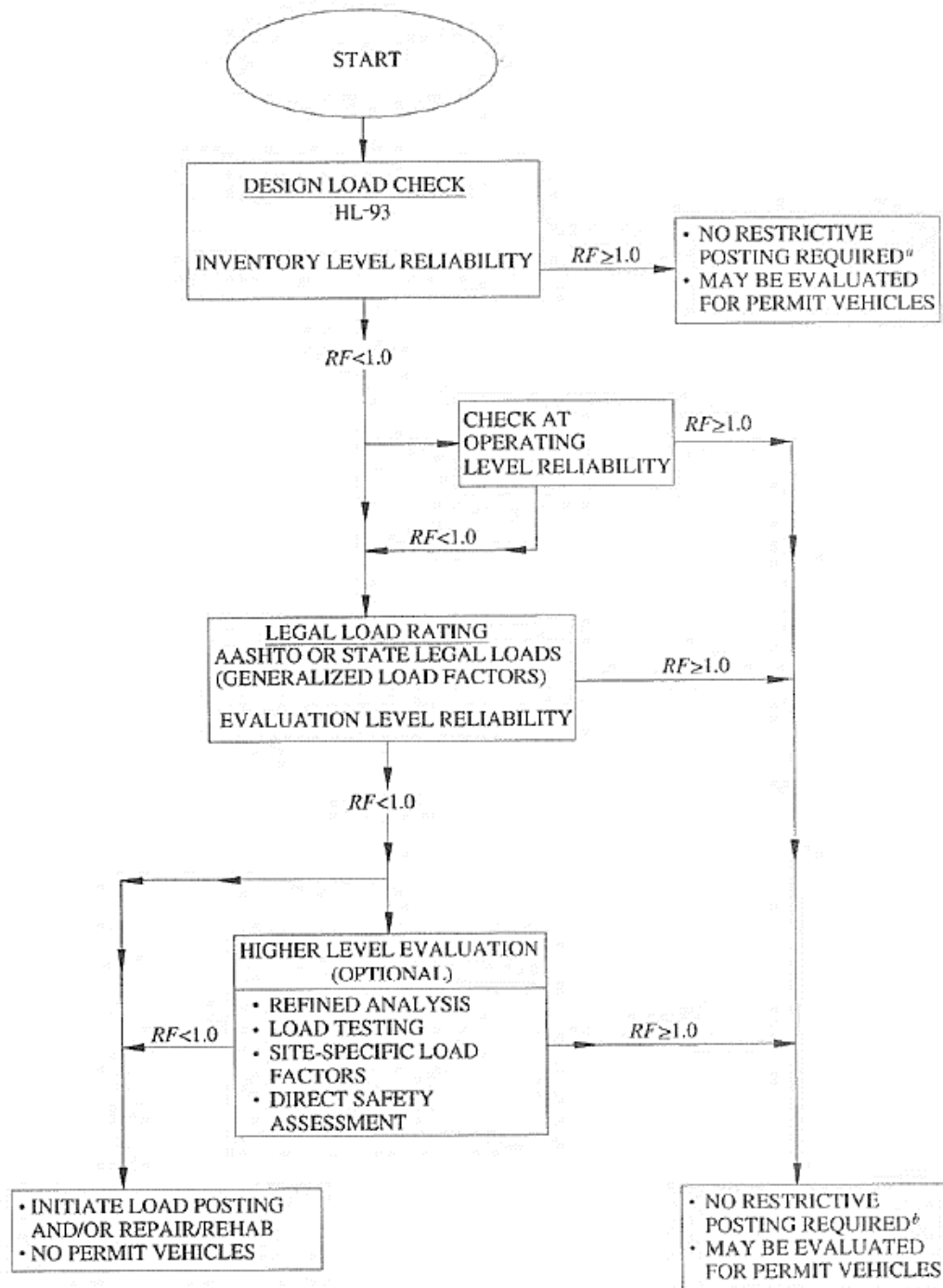


Figure 1. Load and Resistance Factor Rating Flow Chart (AASHTO MBE 3rd Edition)

2.2. General Studies on Load Rating for Steel Truss Bridge without Plans

- 2018 - Washington State Bridge Inspection Manual

If as-built plans are not available, WSDOT suggests load rating to be determined by field evaluation and documented engineering judgment.

- 2018 - Texas Bridge Inspection Manual

Similar to WSDOT, Texas DOT suggests that when a bridge has details not available from plans, then a physical inspection and evaluation may be sufficient to approximate the ratings.

- 2014 - Mississippi DOT Bridge Safety Inspection Policy and Procedure Manual

MDOT stated that, on occasion, a structure may be transferred from a local jurisdiction to state jurisdiction and there will be no plans as to how it was built; for these structures, a rating based on engineering judgment by a qualified engineer familiar with the bridge may be appropriate. A bridge rating based upon engineering judgment should consider.

- 2013 - Iowa Bridge Rating Manual

Iowa DOT stated that in the case of plans are not available, field measurements will be required to determine loads, bridge geometry, and section and material properties. In addition, field evaluation and documented engineering judgment can be used in Operating and Inventory Ratings when severe deterioration is found in the superstructure.

- 2013 - Oregon DOT Bridge Inspection Program Manual

Oregon DOT stated that when bridge plans are not available, the assigned bridge inspector will need to make the field measurements to fully complete the bridge inventory.

- 2013 - Oregon DOT: Methods Used to Obtain Measurements of a Large Truss Bridge with No Plans, Rooper, P.E

In this power point presentation, a professional engineer (PE) from Oregon DOT presented several methods to obtain measurements of a large truss bridge with no plans. His methodologies include 1) hire a consultant to climb the bridge and take measurements, 2) take high resolution photo, and 3) use Light Detection and Ranging (LIDAR). However, the presenter did not explicitly show any results and level of accuracy of each method.

- 2017 – RIDOT Bridge Load Rating Guidelines

RIDOT stated that in the cases where as-built or bid plans do not exist, complete field measurements of the structure will be required to perform the load rating.

2.3. Load Rating Using Site-Specific Weigh-in-Motion (WIM) Data

- 2018- American Association of State Highway and Transportation Officials
Manual for Bridge Evaluation, 3rd ed.

MBE specifies the generalized live load factor for the Strength I limit state for routine commercial traffic. The generalized live load factors are proposed for AASHTO legal loads and state legal loads that have only minor variation from the AASHTO legal loads. MBE indicates that the live load factors in design are assigned to encompass all likely site-to-site variability in loads to maintain a uniform and satisfactory reliability level, which would associate with over conservatism. In evaluation, less strict live load uncertainties are acceptable if traffic that pass through a specific bridge are captured. The site-specific live load factors, by incorporating with the actual traffic data on a certain bridge or within a

certain region, are used to better represent the live load uncertainties for a bridge. The site-specific live load factors can be either lower or higher than the generalized live load factors. The weigh-in-motion (WIM) technology allows the detailed traffic data to be collected with reduced cost. There are variable ways to determine the site-specific live load factor. MBE described two methods in details herein. The first method is a simplified method which is derived from NCHRP Report 454 (Moses, 2001). This approach assumes that the heaviest trucks follow a normal distribution and that 1 in 15 trucks will cross the bridge side-by-side. Only the Gross Vehicle Weight (GVW) of the heaviest 20% trucks Gross Vehicle Weight (GVW) are taken into consideration. The second approaches are studied in NCHRP Report 683 (Sivakumar et al. 2011), which is accompanied with NCHRP Project 12-76. It has proposed a more consistent approach for using WIM data for live load modeling, which takes the actual distribution of the truck traffic data into consideration, including the actual truck configurations and the actual multiple presence percentage. This studies also proposed to use the live load effects instead of the truck weight, including the moment and the shear. Both two approaches are reviewed in the later paragraphs.

- 1999-NCHRP Report 368 Calibration of Load Factors for LRFD Bridge Design Code-Nowak

This report was carried out as a part of the NCHRP Project 12-33. This project aimed at the derivation of the load and resistance factors for the AASHTO *LRFD Bridge Design Specifications*, including various of load models and procedures for determining reliability indices. Regarding the live load model, the real traffic data collected by WIM system is utilized. The maximum positive moment, negative moment, and shear for both simple span and continuous span are calculated for one-lane and two-lane girder bridges. In order to

obtain a consistent mean-to-normal ratio, a new live load model which combines both truck load and uniformly distributed load were developed by using 1975 truck data from the Ontario Ministry of Transportation. Since this project aimed at the state of design, the available data is extrapolated to determine the maximum expected load effects for up to 75 years. In order to extrapolate the future maximum live load effect, it was assumed that the tail end of the maximum live load effect over a certain return period approaches a normal distribution. The live load effects were treated as random variables and were described by cumulative distribution function (CDF). Then the inverse standard normal distribution function, z , can be calculated based on the probability. The plot was finally made for the z value versus the future maximum live load effects over the design load effects.

- 2001-NCHRP Report 454 Calibration of Load Factors for LRFR Bridge Evaluation-Moses

Including the derivations of the live load factors and check criteria for *Manual of Condition Evaluation and Load and Resistance Factor Rating of Highway Bridges*, this report represents the work done by Moses for NCHRP Project 12-46. One of the topics of this report is the calibration of live load factors for legal load ratings for routine traffic and the use of site-specific WIM data. In developing the AASHTO LRFD design specifications, a set of data for very heavy truck that were collected in Ontario was used (Nowak, 1999). In this paper, the Ontario truck data was used again to project the maximum loadings. It was found that for 5000 ADTT, the expected maximum loading in 2 years is 240 kips in 3S2 equivalent for two lanes or 120 kips per lane. In addition, the report also recommended the live load factor for Evaluation Manual as 1.80, which could represent the worst traffic

category, namely 5000 ADTT. Combining the live load factor 1.8 with the expected maximum live load, which is 120 kips for single-lane and 240 kips for double-lane (in 3S2 equivalents), the general expression of the evaluation live load factor for any specific application are shown in Equation 1 and Equation 2.

$$\gamma_{L, one-lane} = 1.8 \times \frac{LL_{\max, one-lane}}{120 \text{ kips}} \quad \text{Equation 1}$$

$$\gamma_{L, two-lane} = 1.8 \times \frac{LL_{\max, two-lane}}{240 \text{ kips}} \quad \text{Equation 2}$$

These two equations were adopted by MBE with small changes. In MBE, while using these equations, the load effects from the 120-kip 3S2 truck are considered rather than the weight.

- 2011-NCHRP Report 683 Protocols for Collecting and Using Traffic Data in Bridge Design- Sivakumar et al.

This report presents the work done for the NCHRP Project 12-76. The study was to develop a set of protocols and methodologies for using available recent truck traffic data to develop and calibrate live-load models for LRFD design. The generalized live load factors for Strength I limit state for the routine commercial vehicle given in MBE were developed under the NCHRP 12-78 project and are based on a target reliability index of 2.5. The protocols include statistical projection methods to obtain the maximum expected live load effects for different return periods. One of the easiest methods, which is also adopted by MBE provisions, provides the results comparable to many other methods including Monte Carlo simulations. This method is based on the assumption that the tail end of the histogram of the maximum load effect over a given return period approaches a Gumbel distribution as the return period increases. The method requires the WIM data to be sufficient that is

assembled over a sufficiently long period of time in order to ensure that the data are representative of the tail end of the truck weight histograms. The use of WIM data for a whole year will satisfy this requirement.

- 2011-Weigh-in-Motion (WIM) Data for Site-Specific LRFR Bridge Load Rating- Nasim Uddin et al.

Alabama DOT, in order to determine the live load factors that can better represent the truck traffic in the state, utilized six WIM sites on state and interstate routes in Alabama. The six selected WIM sites are spread across the state to represent various truck traffic conditions on both the State Highway System and the US Highway System. Data were collected throughout two years. The approach of NCHRP Report 454 (Moses 2001) was used for calibration. The live load factors were calculated based on Oregon DOT and Alabama DOT permit weight classifications, and the results from both classifications are less than those in the LRFR Manual (AASHTO 1994). Compared with the live load factors from the LRFR Manual, the site-specific live load factors are approximately 20% lower for legal vehicles and up to 35% lower for certain permit vehicles. Thus, it is recommended that Alabama DOT consider using the lower live load factors to more accurately load rating the bridges across the state.

- 2011- Load and Resistance Factor Rating (LRFR) in NYS- Ghosn et al.

This report reviewed the current LRFR methodology and recommend state-specific live-load factors for load rating the bridge structures in New York State. The reliability calibration of state-specific live load factors is based on live load models developed using

WIM data collected from several representative New York sites. Five WIM sites that are collecting continuous long-term data were used in this study, but no explanation was provided of why these five locations were chosen. The approach of NCHRP Report 454 (Moses 2001) was proposed to calculate the site-specific live load factor. In addition, the report also recommended to incorporate the protocol proposed by NCHRP 12-76 (Sivakumar, Ghosn & Moses, 2008). The statistical projection methods of the protocols are particularly applicable for determining the live load models necessary for calibrating new LRFR factors and adjusting the load rating equations to represent the live loads observed on New York State bridges.

Chapter III

3. Analysis of Bridges without Plans Using Bridge

Clustering Methodology

3.1. Clustering Methodology

3.1.1. Critical Parameters Related to Load Rating of Steel Truss Bridges

Considering the general load rating equation, the rating factors are determined by the capacity, the dead loads, wearing surface, other permanent loads, and the live load effects. The capacity of a steel structural member is related to the bridge member itself. For steel bridges, the capacity is a function of the bridge geometries, material strength, member sizes. The dead load effects are related to the densities and the sizes of all the bridge components, including the bridge deck, the stringer, the floorbeam, the truss, the diaphragm, the stiffener, and all the other miscellaneous components. The live load effects are affected by the span length and the girder distribution factor (GDF), which is related to the bridge geometry and member sizes. Summarizing all the factors mentioned above, three main parameters are recognized to be influential for the load rating: structure dimensions, material strength, and member sizes. For the bridges without plans, these parameters are all unknown. As a result, the challenge of load rating a steel truss bridge with no plans is to find out these unknown parameters. By incorporating the literature reviews and the actual bridge situations, the solutions to each unknown parameter are shown in Table 1.

Table 1 – Unknown Parameters of Steel Bridge with No Plans

Unknown Parameter	Solutions
Structure Dimensions	Compile inspection report with field measurement
Material strength	Obtain from similar bridges, design codes, and manufactures based on the year of built.
Size of members	1). Estimate based on the bridge clustering 2). Collect data through field inspection

3.1.2. Development of Bridge Clustering Methodology

As illustrated in the above section, among the three unknown parameters, the bridge dimensions can be easily obtained from either the inspection reports or by quick field measurements, and the material strength can be estimated based on the year built. The main challenge is to estimate the member sizes. Typically to load rate a bridge with no plans, the agencies hire engineering consultants to perform field investigations and obtain the required dimensions and size of components. However, it is both time consuming and costly to inspect every element of the structure. Measuring the bridge dimensions on site is relatively easy when the bridge is accessible; however, there are still some locations that are difficult to access, such as the underside of the bridge above the railway. It is sometimes hard to inspect every single element on the bridge. As a result, taking advantage of the existing resources becomes important. Thus, the clustering methodology is proposed to estimate the unknown member sizes based on the bridges that have plans. The load rating procedure incorporates the information from the existing bridges that have plans with the field investigation of the bridges with no plans. To select the suitable bridges for the cluster, the characteristics of the bridge with no plans will need to be deeply investigated, including the following items:

- Year Built: Material strength, such as concrete strength and steel strength, can be estimated based on year built.
- Bridge Geometries: The bridge geometries include both the overall geometries and the member geometries. The overall geometries include the span length, curb-to-curb width, distance between truss centerlines et al. The member geometries mean the geometries for every single member, such as the stringer length, stringer spacing, et al. Those geometries affect both dead load effects and live load effects. For example, the curb-to-curb distance affects the number of lanes that need to be considered; the distance between truss centerlines affects the distribution factors of the truss; the stringer length and spacing affects the distribution factor. The bridge geometries should be investigated as detailed as possible.
- Support conditions: The support condition directly affects the load analysis. The pin-pin support can produce hugely different load effects from the fixed-roller support. As a result, it is important to make sure what the boundary conditions are.
- Truss Type: Given the same applied load, the load distribution could be significantly different if the trusses are in different types.
- Truss Member shape: The different member shape can result in huge difference in the section properties, such as the radius of gyration. As a result, the axial load resistance of the truss member is also greatly affected by the member shape. While estimating the truss members based on the bridges from the cluster, the member shape should be as close as possible. For example, double-angle-shape cannot be used to estimate the truss member with a W-shape section.

After obtaining the characteristics of the bridge needs to be load rated, the similar bridges from the NJDOT bridge inventory that have plans are selected. Theoretically, the bridges selected for the cluster should have as many similarities as possible, but due to the limited number of bridge plans received from NJDOT, the year built and truss type are the priorities of the clustering criteria. The bridges with the same truss type and were built in the same era (roughly plus or minus ten years) as the bridge with no plans are screened out from the NJDOT bridge inventory. In this study, the bridge to be load rated, Structure No. 020033G, was a pony truss bridge that was built in 1996. There are several subsets of the pony truss. The appearance of the specific type of pony truss that is of interest in this study is shown in Figure 2.

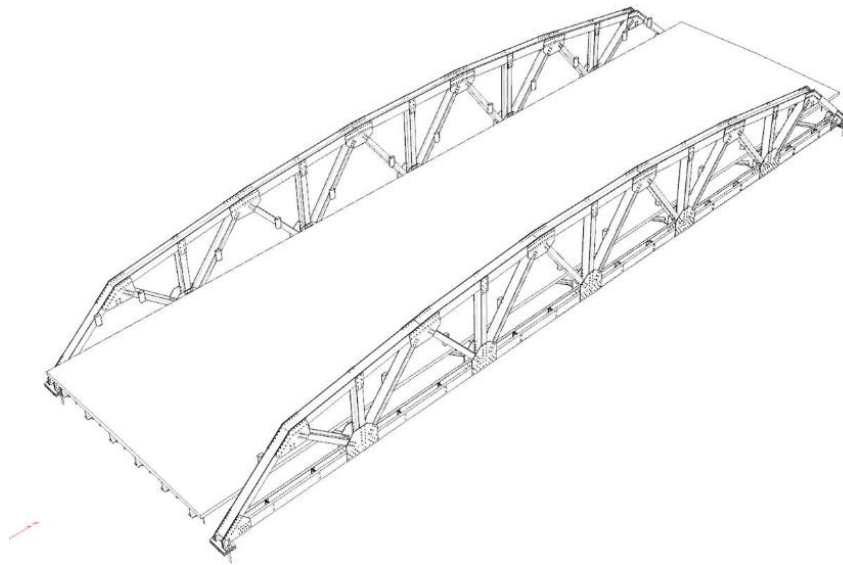


Figure 2. Typical Appearance of the Pony Truss

From the bridge plans that was received from NJDOT, as shown in Table 2, the bridges in red were selected to compose the cluster. These six (6) bridges are all Pony Truss bridge that are built in 1990s and early 2000s.

Table 2 – Steel Truss Floorbeam System Bridges with Plans

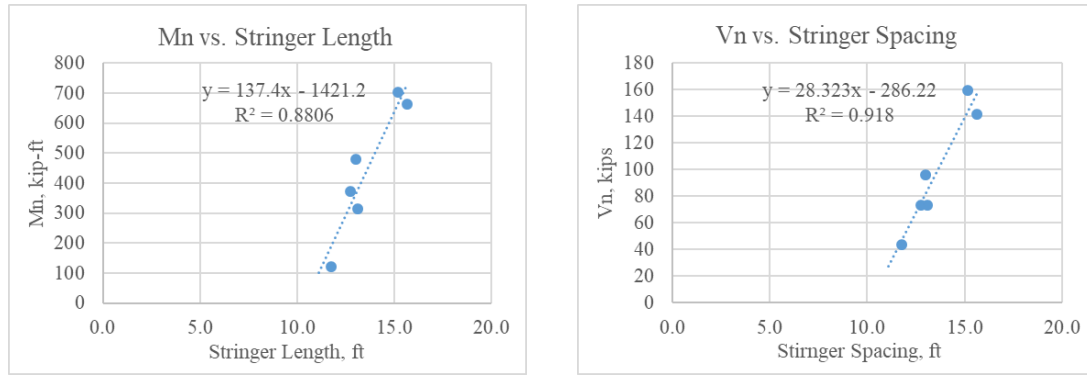
Structure Number	Year built	Design Load	Max Span length (ft)	Truss Type
10XXF76	1901	Unknown	62	Pony w/o verticals
100FC80	1900	Unknown	44	Pratt
1107606	1995	HS25 or greater	66	Pony w/ verticals
1400840	1997	HS25 or greater	67	Pony w/ verticals
1401114	1994	HS25 or greater	101	Pratt
1401119	1994	HS25 or greater	69	Unknown
2101905	1994	HS20+Mod	82	Warren
18D1103	2002	HS25 or greater	63	Pony w/ verticals
125B055	1998	HS20	90	Pony w/ verticals
10XXF48	2003	Unknown	47	Pony w/ verticals
1400724	1991	HS20+Mod	51	Pony w/ verticals

3.2. Analysis of Structural Element Capacity with Respect to Bridge Dimensions

The idea of the clustering methodology is that the member sizes can be estimated based on the parameters that are relatively easy to be obtained. This study focuses on finding the correlations between these influential geometric data and the steel member capacity. Considering the design philosophy, it is easy to come up with the idea that the size of a steel member is affected by some certain parameters, such as span length and tributary area; however, it is important to prove this statement scientifically other than engineering judgment. However, the member size is more or less related to various geometric factors. In order to estimate the member size based on the most-correlated geometric factor, it is important to determine which geometric factor are the most influential. In the following sections, the relationship between the member capacity and each potential geometric factor are plotted, and the influential geometric factors for each structural member are investigated.

3.2.1. Stringer

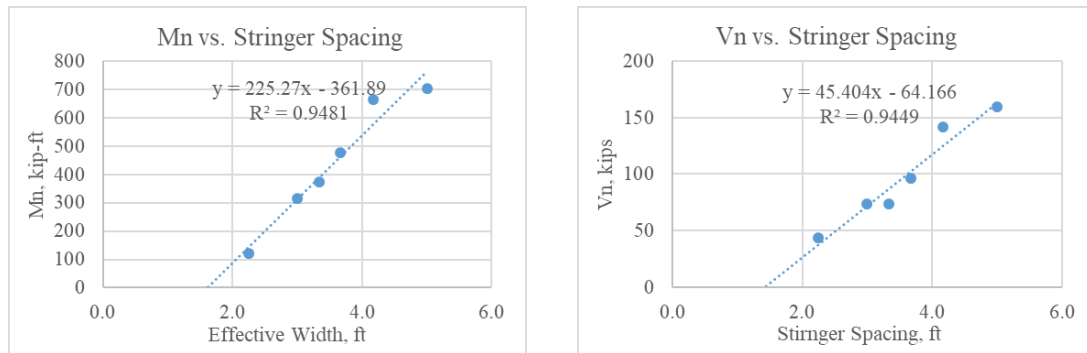
The selection of the stringer size is determined by how much load is resisted by the stringer. In the floorbeam system, the stringer directly supports the bridge deck and is composite with the deck. The dead load is calculated based on the tributary area, which is the stringer length multiply by the effective width. The live load is affected by the girder distribution factor, which is related to both the stringer length and stringer spacing. On balance, stringer length and stringer spacing are the two comparable factors that potentially affect the stringer sizes. For the member that resists bending, both moment capacity and shear capacity are checked. While considering the nominal moment capacity, the effective width for the interior stringer is taken as the stringer spacing, but for the exterior girder, the effective width is normally different from the stringer spacing. For the purpose of having the same sample size of each plot, only the interior stringers are taken into consideration. Figure 4 presents the relationship between the nominal moment and shear capacity versus stringer length. It is shown that both the nominal moment capacity and nominal shear capacity tend to vary linearly with the stringer length. Figure 4 presents the relationship of the nominal moment and shear capacity versus the stringer width. The effect of the slab thickness is also investigated, but there is a strong correlation observed between the slab thickness and the composite nominal capacity. Thus, while looking for a bridge from the bridge cluster to estimate the stringer size, the stringer length and stringer spacing should be considered. In the future, if there are more bridge with plans available, the correlation can be revised and improved.



(a) Nominal Moment Capacity

(b) Nominal Shear Capacity

Figure 3. Stringer Capacity vs. Stringer Length for Steel Truss Bridge



(c) Nominal Moment Capacity

(d) Nominal Shear Capacity

Figure 4. Stringer Capacity vs. Stringer Spacing for Steel Truss Bridge

3.2.2. Floorbeam

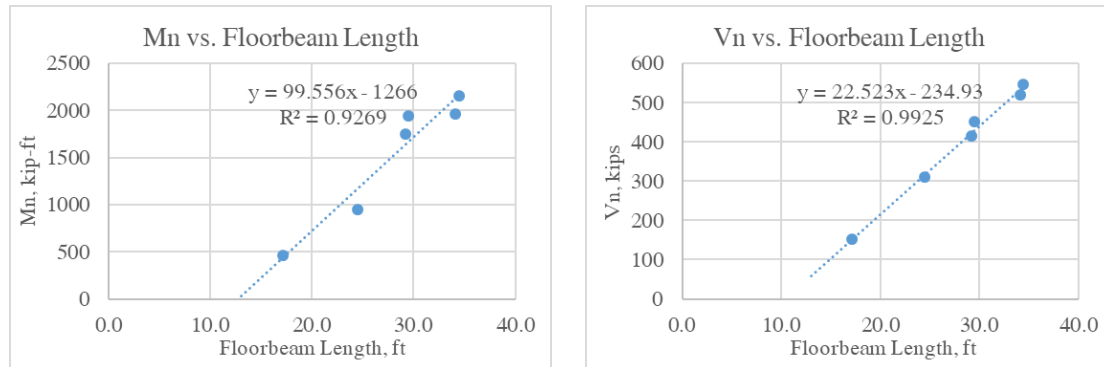
The selection of the floorbeam size is determined by how much load is resisted by the floorbeam. In the floorbeam system, the stringer directly supports the bridge deck, and the stringer is then supported by the floorbeam by either bolt connections or the simple support connection. Similar to the stringer, the dead load resisted by the floorbeam is also related to the tributary area, which is determined by the floorbeam length and the floorbeam spacing. The floorbeam spacing directly determines how many unit loads are transferred from the stringers; the floorbeam length determines the multiplier of the unit loads. As a

result, the floorbeam spacing and the floorbeam length are preliminarily recognized as the influential factors for the floorbeam size. The live loads resisted by the floorbeam are also transferred from the stringers. Accordingly, the girder distribution factors, which is a function of stringer length and stringer spacing, also affect the floorbeam. In addition, since the stringers are supported by the floorbeam, the transferred loads are all acting as concentrated point loads. As a result, the number of stringers, which represents the number of point loads applied, is an influential factor of the capacity.

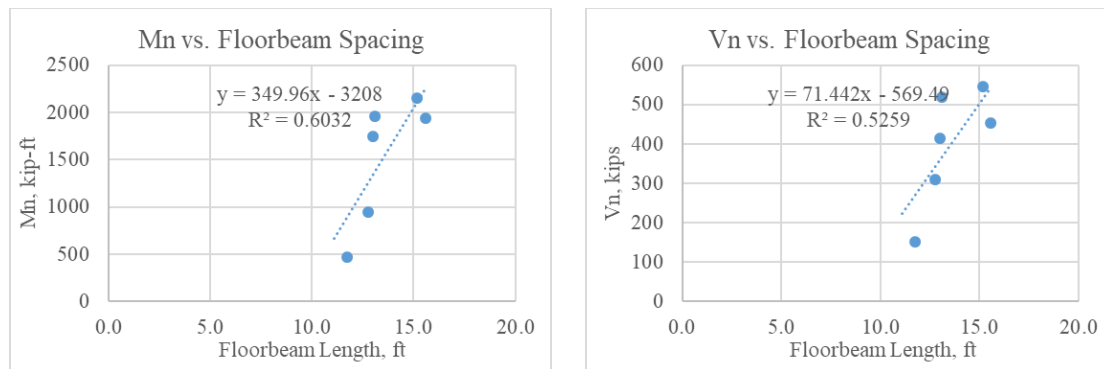
On balance, the floorbeam size is affected by floorbeam length, floorbeam spacing, stringer length, stringer spacing, and number of stringers. However, comparing with the geometries with respect to the floorbeam, the stringer geometries, including the number of stringers, stringer length, and the stringer spacing, normally do not control the selection of the floorbeam size. Thus, it is determined that the floorbeam length and floorbeam spacing are the two comparable factors that can potentially affect the floorbeam resistance. Similar to the stringer, both the moment capacity and the shear capacity are checked.

Figure 5 presents the relationship of the floorbeam nominal moment and shear capacity versus floorbeam length. It is shown that both the nominal moment capacity and nominal shear capacity tend to vary linearly with the stringer length. Figure 6 presents the relationship of the floorbeam nominal moment and shear capacity versus the floorbeam width. Although the data points are relatively more scattered, it is obvious that the floorbeam nominal capacity increases as the spacing increases. In the case that there are only six data points available, it is hard to state that these points are biased or unbiased. In the future, the correlation between the floorbeam capacity and the bridge geometry can be

further investigated if more plans are available. In this study, the unknown floorbeam size will be estimated based on the member length and member spacing.



(a) Nominal Moment Capacity (b) Nominal Shear Capacity
Figure 5. Stringer Capacity vs. Floorbeam Length for Steel Truss Bridge



(c) Nominal Moment Capacity (d) Nominal Shear Capacity
Figure 6. Stringer Capacity vs. Floorbeam Spacing for Steel Truss Bridge

3.2.3. Truss Member

For the steel truss bridge with the floorbeam system, the trusses resist all the loads from the bridge. As shown in Figure 7, the weight of the bridge deck and the truck load are carried by the stringers into the floor beam, and then the floor beam carries these loads to the truss at the node point. As a result, all the geometric information that affects the amounts of loads applied to the node point should be considered. Firstly, the deck width is

recognized as influential because the deck width can be effectively related to the the dead load of the bridge. Also, the distance between the truss centerlines is also important since it affects the live load distribution of the trusses. Since the deck width is always close to the distance between the truss centerlines, only the distance between the truss centerlines is used for investigating the correlation between the member capacity and the bridge geometry. In addition, member length also affects the member resistance because the member length may change the slenderness of the truss member, which act as a column somehow. Moreover, the bridge span length of the bridge may affect the overall load effects. In all, the distance between truss centerlines, member length, and the bridge span length are studies in this paper.

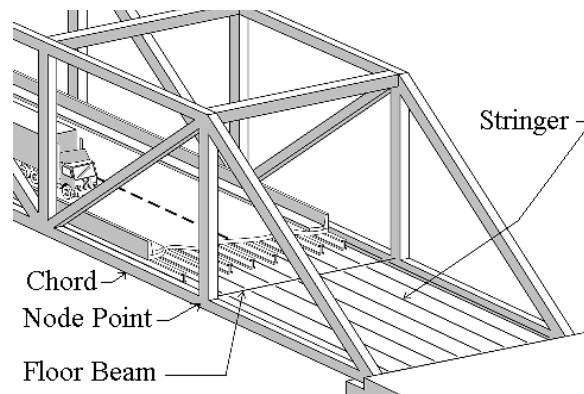


Figure 7. Configuration of the Typical Steel Truss Through Bridge

For a truss bridge, the truss members are mostly pin-pin connected each other by the gusset plates, so that it is assumed that the truss members are subjected to axial load only. The truss member can be either in tension or in compression. As will illustrated in detail in the later chapter, the LRFD Design codes have provided clear instructions on calculating the nominal resistance of the member that is subjected to the axial load. Based on the LRFD provisions, the nominal tensile resistance shall be taken as the lesser of the nominal tensile resistance for yielding in gross section and the nominal tensile resistance for rupture in net

section. Both two cases are directly related to the cross-sectional area of the truss member. Thus, in order to investigate the relationship between the nominal tensile resistance and the bridge geometries, the cross-sectional area is used to represent the nominal tensile capacity. The nominal compressive resistance is a function of material property, cross-sectional area, and column slenderness term. Further, the column slenderness term is a function of material properties, radius of gyration, and member length. All of the cross-sectional area, radius of gyration, and the member length affect the nominal compressive capacity, but only the cross-sectional area is the direct multiplier of the nominal compressive capacity. Besides, considering that the expressions for the column slenderness term are different for members with different shapes, it is not proper to derive any correlations with respect to the column slenderness factor. As a result, for the purpose of finding the correlations between the member capacity and the bridge geometries, the member nominal capacity is represented by the cross-sectional area.

On balance, both of the nominal tensile resistance and the nominal compressive resistance are represented by the cross-sectional area. In this study, as shown in Figure 2, the specific truss type is studied. For this type of truss, there are top chords, bottom chords, diagonals, and vertical members, but the vertical members are zero force members, so that the size of the vertical member is not investigated. Figure 8 presents the relationship between the cross-sectional area of the truss members and the bridge width, which is the distance between the truss centerlines. Figure 9 shows the relationship between truss member cross-sectional areas and the member length. Figure 10 shows the relationship between the truss member cross-sectional area and the bridge span length. Due to the limit number of data

points, it is difficult to predict the best-fit function type, but it can be noticed that the member cross-sectional area increases with all the three geometric factors. It is proposed that in the future study, the correlations should be further investigated if there are more bridge plans available.

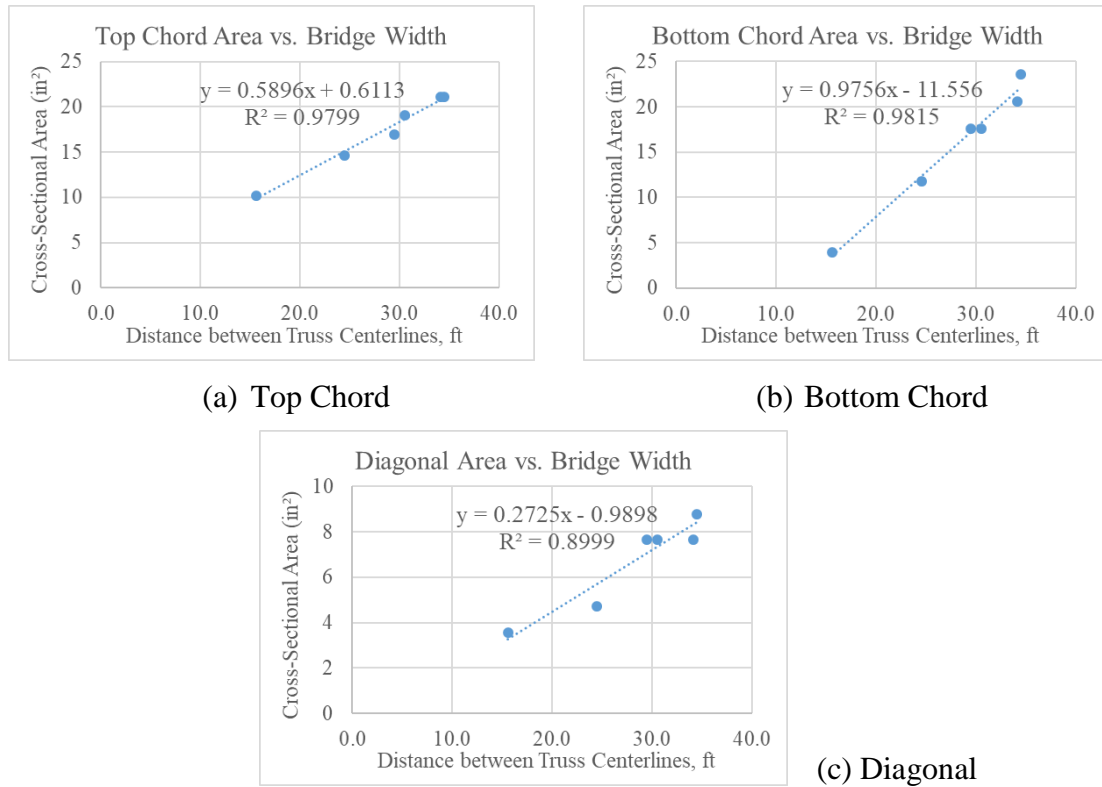
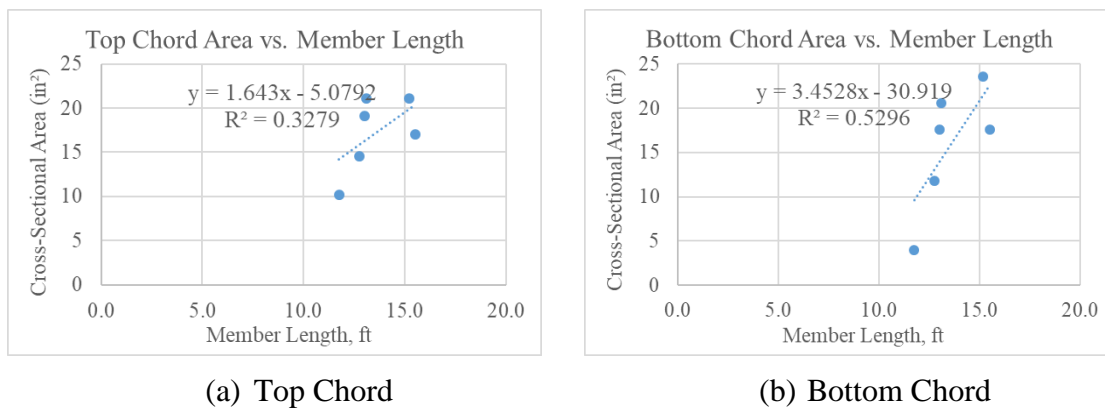
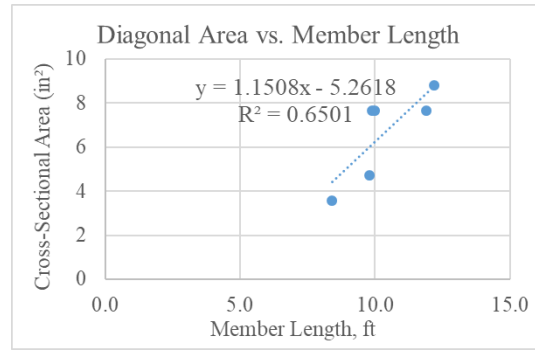


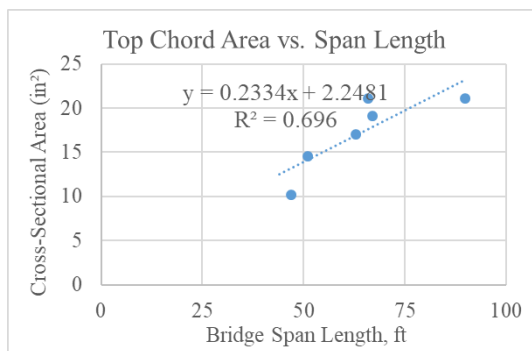
Figure 8. Truss Member Cross-Sectional Area vs. Distance between Truss Centerlines



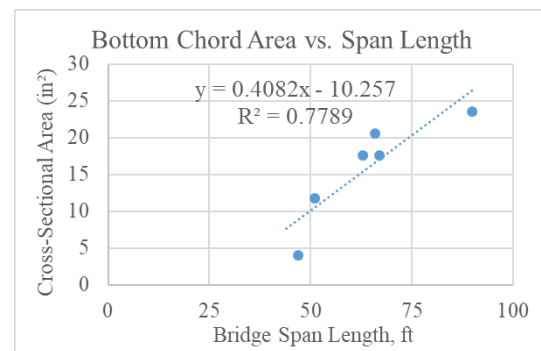


(c) Diagonal

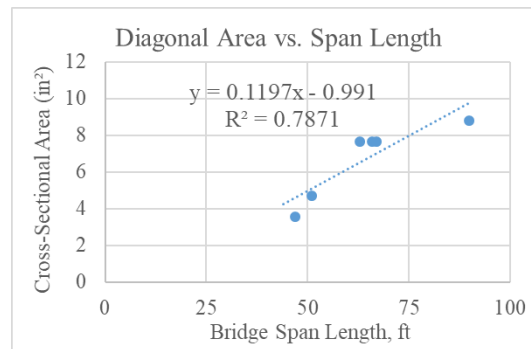
Figure 9. Truss Member Cross-Sectional Area vs. Member Length



(a) Top Chord



(b) Bottom Chord



(c) Diagonal

Figure 10. Truss Member Cross-Sectional Area vs. Bridge Span Length

3.3. Obtaining the Member Sizes of the Bridge without Plans

3.3.1. Estimation of the Member Size Using Clustering Method

By incorporating with the previous sections, the correlations between the member capacity and the bridge geometries are confirmed. For each structural member, there are various

influential factors that would affect the member size, as shown in Table 3. The ideal scenario is that an equation can be derived from the correlations to estimate the member capacity in the function of the correlative geometric factors; however, due to the limit number of data points, the conclusive equations cannot be derived. In this study, while estimating the unknown member sizes, all the correlative geometric factors are incorporated.

Table 3 – Summary of the Correlative Factors

Structural Element	Correlative Factor
Stringer	Stringer spacing; stringer length
Floorbeam	Floorbeam spacing; floorbeam length
Truss Member	Bridge width (distance between truss centerlines); member length; bridge span length

Based on the bridge inspection report, the target bridge to be load rated has the stringer with 13.5 ft length and 3.5 ft spacing. The stringer sections of the bridges with known plans are summarized in Table 4. In order to select the most probable stringer section of the target bridge, the selected reference bridge should have a similar stringer length and stringer spacing. As shown in Table 4, two bridges in red have the similar geometries. In the case that more than one bridge have similar geometries as the target bridge, the one with the smaller section is considered due to the conservative concern. In this cluster, both two bridges have the same stringer size, W12x30. Thus, the stringer size of the target bridge is estimated as W12x30.

Table 4 – Summary of the Stringer Sections

Structure Number	Stringer	Stringer Spacing	Stringer Length
020033G (No Plan)	-	3.5 ft	13.5 ft
10XXF48	W 8x18	2.3 ft	11.8 ft
1400840	W14x34	3.7 ft	13.0 ft
1107606	W 12x30	3.0 ft	13.1 ft
18D1103	W18x40	4.2 ft	15.6 ft
125B055	W18x50	5.0 ft	15.2 ft
1400724	W12x30	3.3 ft	12.8 ft

Based on the bridge inspection report, the target bridge has the floorbeam with the length of 23.5 ft and spacing of 13.5 ft. The floorbeam sections of the bridges with known plans are summarized in Table 5. Among all the six bridges from the cluster, only one bridge is recognized to be proper to become the reference bridge that has both similar floorbeam length and similar floorbeam spacing. All the other bridges only have one similarity or even no similarity, potentially leading to inaccurate prediction. Thus, the stringer size of the bridge with no plan is finally estimated as W24x94.

Table 5 – Summary of the Floorbeam Sections

Structure Number	Floorbeam	Floorbeam Spacing	Floorbeam Length
020033G (No Plan)	-	13.5 ft	23.5 ft
10XXF48	W16x67	11.8 ft	17.2 ft
1400840	W27x146	13.0 ft	29.1 ft
1107606	W33X141	13.1 ft	34.1 ft
18D1103	W27x161	15.6 ft	29.5 ft
125B055	W33x152	15.2 ft	34.4 ft
1400724	W24x94	12.8 ft	24.5 ft

Based on the bridge inspection report, the bridge width of the target bridge to be load rated is about 24.5 ft, and bridge span length of 107 ft. The truss sections of the bridges with known plans are summarized in Table 6. Recalling that as illustrated in the previous section,

the truss member shape is also an important factor to be considered. While selecting the reference bridge, the shape of the member shape should be as closer to the target bridge as possible. For the target bridge to be load rated, the top chords, diagonals, and vertical members are all made of W-shape steel, and the bottom chords are made of 2-C or 2-MC shape. It is observed from Table 6 that all of the bridges use the same steel shape as the target bridge except the bridge with Structure No. 10XXF48. The ideal scenario of selecting the reference bridge is that there is at least one bridge that has all the correlative geometries similar to the target bridge. However, according to Table 6, among the six bridges in the cluster, none of the bridges is similar to the target bridge in all the three aspects. As a result, the bridge width is primarily considered because the bridge width presents the strongest correlation with the live load effects based on the current six data points. One bridge is screened out which has the same bridge width as the target bridge. However, the reference bridge has much shorter span length as the target bridge. Thus, the estimation results should be much conservative. The estimation can be more accurate if there are more bridges with plans available. The more bridges have, the more possibility that there exist bridges that have all three aspects similar to the target bridge. In this study, the final results of the estimation of the truss members are based on the bridge with Structure No. 1400724, as marked in red in the table below.

Table 6 – Summary of the Truss Member Sections

Structure Number (Bridge Width) (Span Length)	Top Chord	Bot Chord	Vertical	Diagonal
020033G (No Plan) (24.5 ft) [107 ft]	- (13.5 ft)	- (13.5 ft)	- (11 ft)	- (11.2 ft)
10XXF48	2L's 6x6x7/16	2L's 5x3 1/2 x 1/2	2L's 2 1/2 x 2 1/2 x 5/16	2L's 3x3x5/16
1400840 (29.1 ft) [67 ft]	W12x65 (13.0 ft)	2-C12x30 (13.0 ft)	W12x26 (7.5 ft)	W12x26 (8.9 ft)
1107606 (34.1 ft) [66 ft]	W12x72 (13.1 ft)	2-MC12x35 (13.1 ft)	W12x26 (7.5 ft)	W12x26 (10.0 ft)
18D1103 (29.5 ft) [63 ft]	W12x58 (15.6 ft)	2-C10X30 (15.6 ft)	W12x26 (9 ft)	W12x26 (11.9 ft)
125B055 (34.4 ft) [90 ft]	W12x72 (15.2 ft)	2-MC12x40 (15.2 ft)	W12x30 (9.5 ft)	W12x30 (12.2 ft)
1400724 (24.5 ft) [51 ft]	W12x50 (12.75')	MC12x40 (12.75')	W12x26 (7.5')	W12x16 (9.84')

3.3.2. Validation of the Clustering Results by Field Inspection

As shown in Figure 11, Structure No. 020033G is a single-span simply-supported Pony Truss bridge with a sidewalk on one side. It locates on Glen Gray Road over Ramapo River and is about half mile west to U.S. Route 202. Although the bridge locates near the U.S. Highway, it is not likely to sustain the high-volume of truck traffic, because the bridge locates at a rural area near a residential area. This bridge is currently not posted for a restricted load limit.



(a) Location of Structure No. 020033G



(b) General View of Structure No. 020033G

Figure 11. Overview of Structure No. 020033G

In order to validate the accuracy of the clustering methodology, the field inspection was performed. The truss members, as shown in Figure 11 (b), could be directly measured on the sidewalk. The abutment of the bridge abutment was constructed on the shallow river bank, which is also easy to access. Thus, the underside of the bridge was also approachable,

so that the stringer and the floorbeam were also measured. Multiple inspection details are shown in Figure 12.



(a) Inspection of the Stringer



(b) Inspection of the Floorbeam



(c) Inspection of the Truss Member



(d) Inspection of the Truss Member

Figure 12. Field Inspection on structure No. 030033G

In order to validate the accuracy of the clustering method, the field inspection results as well as the clustering results are shown together in Table 7.

Table 7 – Comparison between Field Inspection and Clustering Method

	Field Inspection		Clustering Method	
Stringer	W12x35		W12x30	
Floorbeam	W24x94		W24x94	
Truss Member	Top chord	W12x58	Top chord	W12x50
	Bottom chord	2-MC15x40	Bottom chord	2-MC12x40
	Diagonal	W12x30	Diagonal	W12x16

According to the above table, the clustering method provides the section sizes that are very close to the actual member sizes. The estimated stringer section is relatively smaller than the actual stringer section. Recalling that the reference bridge has relatively smaller stringer spacing than the bridge with no plan, this result makes sense. The estimated floorbeam section is the same as the field measurement result. This is because for both the bridge with no plans and the reference bridge in the cluster have almost the same floorbeam length. This proves that the floorbeam section is greatly affected by the floorbeam length. The estimated truss members are generally smaller than the actual truss member sizes. The possible reason, as mentioned above, is that the reference bridge has much shorter span length than the target bridge. Another reason can be possibly account on the existence of the sidewalk of the target bridge. If there is a sidewalk on the truss bridge, both the dead load and the live load from the sidewalk are usually transferred to the node point of the truss. The bridge with no plans has sidewalk on one-side, whereas the reference bridge from the bridge cluster does not have a sidewalk. As a result, it is reasonable that the target bridge has bigger truss members. Whether the bridge has sidewalk or should become a criterion for clustering the bridge inventory, but in the case that there is limited number of bridges with plans, this criterion was not considered in this thesis.

Chapter IV

4. Load Rating of the Bridge with No Plans

4.1. Proposed Procedures for Load Rating the Steel Truss Bridge with No Plans

The proposed procedure to load rate steel truss bridges with no plans is shown in Figure 13.

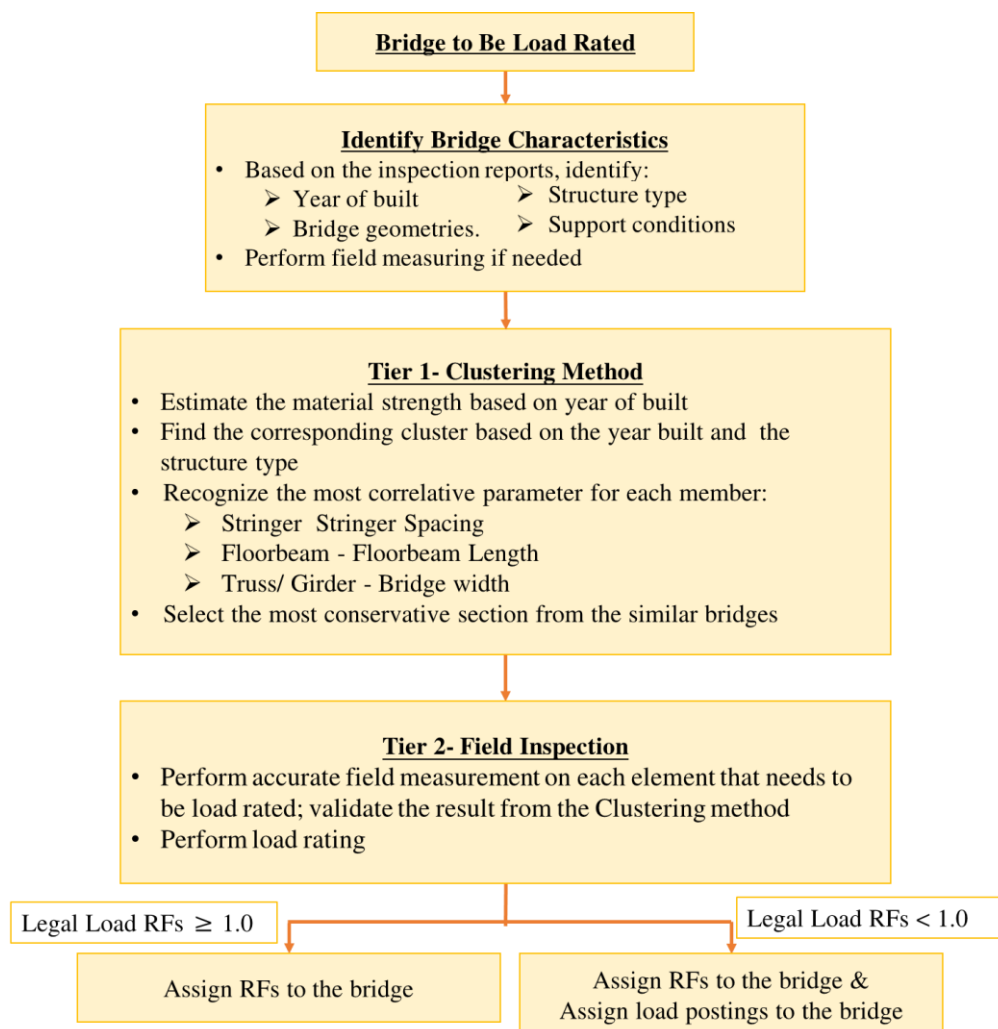


Figure 13. Guideline for Load Rating the Steel Truss Bridges without Plans

4.2. Analysis of Member Capacity

4.2.1. Stringer Resistance

The stringers are composite with the concrete deck. The concrete is transformed into an equivalent area of steel by dividing the area of the slab by modular ratio. Live load plus impact stresses are carried by the composite section using a modular ratio of n . To account for the effect of creep, superimposed dead-load stresses are carried by the composite section using a modular ratio of $3n$ (LFRD Design, 2017).

The modular ratio is determined using

$$n = \frac{E_B}{E_D} \quad \text{Equation 3}$$

$$E_B = 33000(w_c)^{1.5} \sqrt{f'_c} \quad \text{Equation 4}$$

The nominal flexure resistance M_n of the steel beam is a function of plastic moment, M_p :

If $D_p \leq 0.1D_t$,

$$M_n = M_p \quad \text{Equation 5}$$

where, D_t = depth of composite section, and

D_p =newtral axis of composite section

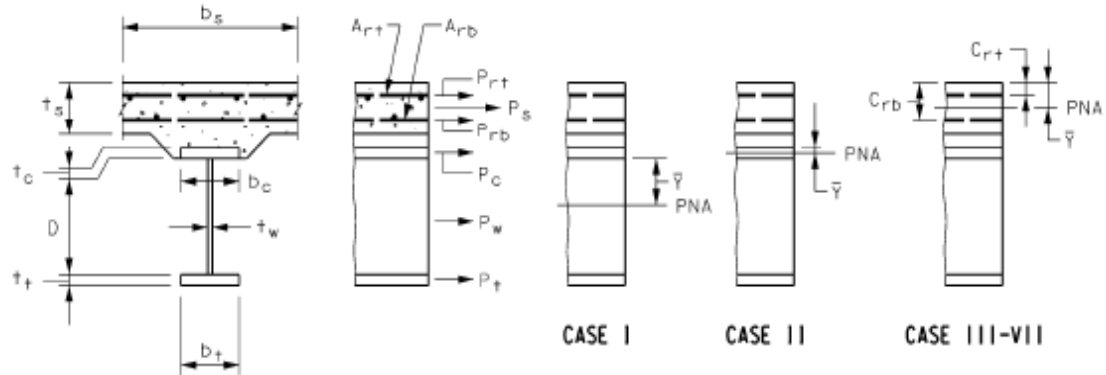
Otherwise,

$$M_n = M_p \left(1.07 - 0.7 \frac{D_p}{D_t}\right) \quad \text{Equation 6}$$

The calculation of M_p shall follow Table 8 as per AASHTO MBE provisions.

Table 8 – Calculation of \bar{Y} and M_p for Sections in Positive Flexure
(AASHTO MBE, 2018)

Case	PNA	Condition	\bar{Y} and M_p
I	In Web	$P_t + P_w \geq P_c + P_s + P_{rb} + P_n$	$\bar{Y} = \left(\frac{D}{2}\right) \left[\frac{P_s - P_c - P_s - P_n - P_{rb}}{P_w} + 1 \right]$ $M_p = \frac{P_w}{2D} \left[\bar{Y}^2 + (D - \bar{Y})^2 \right] + [P_s d_s + P_n d_n + P_{rb} d_{rb} + P_c d_c + P_t d_t]$
II	In Top Flange	$P_t + P_w + P_c \geq P_s + P_{rb} + P_n$	$\bar{Y} = \left(\frac{t_s}{2}\right) \left[\frac{P_w + P_t - P_s - P_n - P_{rb}}{P_c} + 1 \right]$ $M_p = \frac{P_c}{2t_s} \left[\bar{Y}^2 + (t_s - \bar{Y})^2 \right] + [P_s d_s + P_n d_n + P_{rb} d_{rb} + P_w d_w + P_t d_t]$
III	Concrete Deck, Below P_{rb}	$P_t + P_w + P_c \geq \left(\frac{c_{rb}}{t_s}\right) P_s + P_{rb} + P_n$	$\bar{Y} = (t_s) \left[\frac{P_c + P_w + P_t - P_n - P_{rb}}{P_s} \right]$ $M_p = \left(\frac{\bar{Y}^2 P_s}{2t_s} \right) + [P_n d_n + P_{rb} d_{rb} + P_c d_c + P_w d_w + P_t d_t]$
IV	Concrete Deck, at P_{rb}	$P_t + P_w + P_c + P_{rb} \geq \left(\frac{c_{rb}}{t_s}\right) P_s + P_n$	$\bar{Y} = c_{rb}$ $M_p = \left(\frac{\bar{Y}^2 P_s}{2t_s} \right) + [P_n d_n + P_c d_c + P_w d_w + P_t d_t]$
V	Concrete Deck, Above P_{rb} Below P_n	$P_t + P_w + P_c + P_{rb} \geq \left(\frac{c_n}{t_s}\right) P_s + P_n$	$\bar{Y} = (t_s) \left[\frac{P_{rb} + P_c + P_w + P_t - P_n}{P_s} \right]$ $M_p = \left(\frac{\bar{Y}^2 P_s}{2t_s} \right) + [P_n d_n + P_{rb} d_{rb} + P_c d_c + P_w d_w + P_t d_t]$
VI	Concrete Deck, at P_n	$P_t + P_w + P_c + P_{rb} + P_n \geq \left(\frac{c_n}{t_s}\right) P_s$	$\bar{Y} = c_n$ $M_p = \left(\frac{\bar{Y}^2 P_s}{2t_s} \right) + [P_{rb} d_{rb} + P_c d_c + P_w d_w + P_t d_t]$
VII	Concrete Deck, Above P_n	$P_t + P_w + P_c + P_{rb} + P_n < \left(\frac{c_n}{t_s}\right) P_s$	$\bar{Y} = (t_s) \left[\frac{P_{rb} + P_c + P_w + P_t + P_n}{P_s} \right]$ $M_p = \left(\frac{\bar{Y}^2 P_s}{2t_s} \right) + [P_n d_n + P_{rb} d_{rb} + P_c d_c + P_w d_w + P_t d_t]$



The nominal shear resistance is straightforward as shown below:

$$V_n = V_{cr} = CV_p \quad \text{Equation 7}$$

$$\text{where, } V_p = 0.58F_{yw}D_{tw} \quad \text{Equation 8}$$

The C value shall be calculated using Equation 9, Equation 10, or Equation 11.

- If $\frac{D}{t_w} \leq 1.12 \sqrt{\frac{Ek}{F_{yw}}}$, then:

$$C = 1.0 \quad \text{Equation 9}$$

- If $1.12 \sqrt{\frac{Ek}{F_{yw}}} < \frac{D}{t_w} \leq 1.40 \sqrt{\frac{Ek}{F_{yw}}}$, then:

$$C = \frac{1.12}{\frac{D}{t_w}} \sqrt{\frac{Ek}{F_{yw}}} \quad \text{Equation 10}$$

- If $\frac{D}{t_w} > 1.40 \sqrt{\frac{Ek}{F_{yw}}}$, then:

$$C = \frac{1.57}{\left(\frac{D}{t_w}\right)^2} \left(\frac{Ek}{F_{yw}}\right) \quad \text{Equation 11}$$

The bridge with no plans has the stringer size of W12x35 and 6-in-thick concrete deck. By checking the conditions in Table 8, the interior composite stringer belongs to Case V, and the exterior composite stringer belongs to Case III. The nominal flexure resistance of the interior stringer and the exterior stringer are calculated as 380.38 kip-ft and 341.11 kip-ft, respectively. The nominal shear resistance for the interior stringer and exterior stringer are both 104.23 kips.

4.2.2. Floorbeam Resistance

The floorbeams are not directly connected with the bridge deck. Thus, when analyzing the properties of the floorbeams, they are considered as non-composite sections. Similar to the stringer, the plastic moment M_p is calculated based on Table 8. Since the section is non-composite, only Case I and Case II are considered. The nominal flexure resistance, as specified in *LRFD Design Manual*, is taken as the smaller of the local buckling resistance and lateral torsional buckling resistance.

The local buckling resistance can be calculated as follow:

$$\begin{aligned} M_{nc} &= R_{pc} M_{yc} \\ &= \frac{M_p}{M_{yc}} \times M_{yc} \\ &= M_p \end{aligned} \quad \text{Equation 12}$$

The calculation of the lateral torsional buckling resistance can be followed:

- If $L_b \leq L_r$, then:

$$M_n = C_b \left[M_p - (M_p - 0.7 F_y S_x) \left(\frac{L_b - L_p}{L_r - L_p} \right) \right] \leq M_p \quad \text{Equation 13}$$

- If $L_b > L_r$, then:

$$M_n = F_{cr} S_x \leq M_p \quad \text{Equation 14}$$

$$\text{where, } r_t = \frac{b_{fc}}{\sqrt{12 \left[1 + \frac{1}{3} \left(\frac{D_c t_w}{b_{fc} t_{fc}} \right) \right]}} \quad \text{Equation 15}$$

$$L_p = 1.0 r_t \sqrt{\frac{E}{F_{yc}}} \quad \text{Equation 16}$$

$$L_r = 1.95r_t \frac{E}{F_{yr}} \sqrt{\frac{J}{S_{xc}h}} \sqrt{1 + \sqrt{1 + 6.76\left(\frac{F_{yr}}{E} - \frac{S_{xc}h}{J}\right)^2}} \quad \text{Equation 17}$$

The calculation of nominal shear resistance is the same as the stringer. Equation 7 through Equation 11 are also applied to the nominal shear resistance of the floorbeam.

For the bridge with no plans, both the local buckling resistance and the lateral torsional buckling resistance equal to the plastic moment. The nominal flexure resistance of the floorbeam is calculated as 946.07 kip-ft. The nominal shear resistance is 309.9 kips.

4.2.3. Truss Member Resistance

The truss members can resist both compressional axial force or tensile axial force.

Check limiting slenderness ratio:

$$\frac{kl}{r} < 120 \text{ for main members OK}$$

$$K = 0.875 \text{ for pinned ends}$$

Nominal compressive resistance is calculated by the following procedure:

Column slenderness term λ is defined as:

$$\lambda = \left(\frac{kl}{r_s \pi}\right)^2 \frac{F_y}{E} = \left(\frac{kl/r}{\pi}\right)^2 \frac{F_y}{E} \quad \text{Equation 18}$$

Check Limiting Width/Thickness Ratios:

$$\frac{b}{t} \leq \lambda_r \quad \text{Equation 19}$$

$$\lambda_r = \text{Width to thickness ratio limit as specified in Table 13}$$

The value of k and b can also be found in Table 9.

$$P_n = -0.66^{\lambda} F_v A_s \quad \text{Equation 20}$$

$$P_r = \phi_c P_n = 0.9 P_n \quad \text{Equation 21}$$

Table 9 – Plate Buckling Coefficients and Width of Plates for Axial Compression
(AASHTO LRFD, 2017)

Plates Supported along One Edge (Unstiffened Elements)	k	b
Flanges of Rolled I-, Tee, and Channel Sections; Plates Projecting from Rolled I-Sections; and Outstanding Legs of Double Angles in Continuous Contact	0.56	• Half-flange width of rolled I- and tee sections
		• Full-flange width of channel sections
		• Distance between free edge and first line of bolts or welds in plates
		• Full width of an outstanding leg for double angles in continuous contact
Stems of Rolled Tees	0.75	• Full depth of tee
Outstanding Legs of Single Angles; Outstanding Legs of Double Angles with Separators; and All Other Unstiffened Elements	0.45	• Full width of outstanding leg for single angle or double angles with separators
		• Full projecting width for all others
Plates Supported Along Two Edges (Stiffened Elements)	k	b
Flanges and Webs of Square and Rectangular Built-Up Box Sections and HSS; and Nonperforated Flange Cover Plates	1.40	• Distance between adjacent lines of bolts or welds in flanges of built-up box sections
		• Distance between adjacent lines of bolts or clear distance between flanges when welds are used in webs of built-up box sections
		• Clear distance between webs or flanges minus inside corner radius on each side for HSS. Use the outside dimension minus three times the appropriate design wall thickness specified in Article 6.12.2.2.2 if the corner radius is not known
		• Distance between lines of welds or bolts for flange cover plates
Webs of I- and Channel Sections; and All Other Stiffened Elements	1.49	• Clear distance between flanges minus the fillet or corner radius at each flange for webs of rolled I- and channel sections
		• Distance between adjacent lines of bolts or clear distance between flanges when welds are used for webs of built-up I- and channel sections
		• Clear distance between edge supports for all others
Perforated Cover Plates	1.86	• Clear distance between edge supports; see also the paragraph at the end of Article 6.9.4.3.2

Nominal tension resistance is taken by the less of the yielding limit state and fracture limit state.

For the yielding over the gross area, the nominal tension resistance is taken as:

$$P_r = \phi_y F_y A_g = 0.95 F_y A_g \quad \text{Equation 22}$$

For the fracture at the net area, the nominal tension resistance is taken as:

$$P_r = \phi_u F_u A_n R_p U \quad \text{Equation 23}$$

$$U = 1.0$$

$$\phi_u = 0.80 \text{ (tension, fracture in net section)}$$

$$R_p = 1.0$$

In order to determine whether the truss member is in compression or in tension, a 2D model using SAP2000 was used to investigate the load effects of each truss member. The dead load was applied at each node point. As shown in Figure 14, for this bridge, all of the top chords are compression members; all the bottom chord member are tension members; the diagonals have both compression members and tension members. As a result, only the nominal compressive resistance needs to be considered for the top chord; only the nominal tensile resistance needs to be considered for the bottom chord. For the diagonal member, both compressive and tensile resistance need to be checked. The vertical members are not evaluated in this study because the vertical member is a zero-force member.

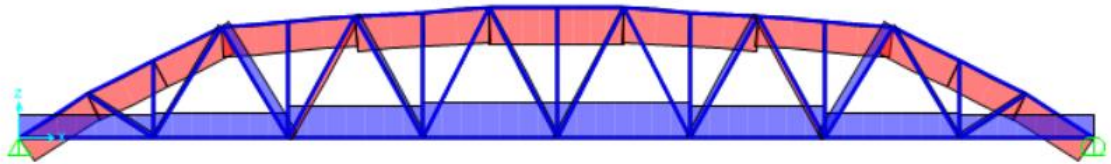


Figure 14. Dead Load Effects of the Bridge with No Plan (SN. 020033G)

The top chord is a rolled I-section, so that the first category in Table 9 can be applied. The nominal compressive resistance of the top chord is calculated as 726.01 kips. Due to the limited information regarding the truss connection, the net area of tension members is hard to be calculated. The nominal tensile resistance is calculated based on the gross area yielding limit state, and the resistance of the bottom chord is 1121.00 kips. The diagonal member is also made of rolled I-section. The nominal compressive resistance and tensile resistance are 372.31 kips and 471.53 kips, respectively.

4.3. Live Load Effects using AASHTO GDF Equations

The *AASHTO LRFD Bridge Design Specifications* have provided the girder distribution factor (GDF) for beam-slab bridge to count for how many fractions of the load effects caused by one truck is taken by one girder. The girder distribution factors take both moment and shear into consideration and will be illustrated in this section. With the GDF, the load effect each girder is resisting can be estimated by multiplying the global live load effects with the GDF. The GDF for moment in the interior beam, the GDF for shear in the interior beam, the GDF for moment in the exterior beam, and the GDF for shear in the exterior beam are shown through Table 10 to Table 13.

Table 10 – Distribution of Live Loads for Moment in Interior Beam
(AASHTO LRFD *Bridge Design Specifications*, 2017)

Type of Superstructure	Applicable Cross-Section from Table 4.6.2.2.1-1	Distribution Factors	Range of Applicability
Concrete Deck, Filled Grid, Partially Filled Grid, or Unfilled Grid Deck Composite with Reinforced Concrete Slab on Steel or Concrete Beams; Concrete T-Beams, T- and Double T-Sections	a, e, k and also i, j if sufficiently connected to act as a unit	One Design Lane Loaded: $0.06 + \left(\frac{S}{14}\right)^{0.4} \left(\frac{S}{L}\right)^{0.3} \left(\frac{K_g}{12.0 L t_s^3}\right)^{0.1}$	$3.5 \leq S \leq 16.0$ $4.5 \leq t_s \leq 12.0$ $20 \leq L \leq 240$ $N_b \geq 4$
		Two or More Design Lanes Loaded: $0.075 + \left(\frac{S}{9.5}\right)^{0.6} \left(\frac{S}{L}\right)^{0.2} \left(\frac{K_g}{12.0 L t_s^3}\right)^{0.1}$	$10,000 \leq K_g \leq 7,000,000$
		use lesser of the values obtained from the equation above with $N_b = 3$ or the lever rule	$N_b = 3$

Table 11 – Distribution of Live Loads for Shear in Interior Longitudinal Beam
(AASHTO LRFD *Bridge Design Specifications*, 2017)

Type of Superstructure	Applicable Cross-Section from Table 4.6.2.2.1-1	One Design Lane Loaded	Two or More Design Lanes Loaded	Range of Applicability
Concrete Deck, Filled Grid, Partially Filled Grid, or Unfilled Grid Deck Composite with Reinforced Concrete Slab on Steel or Concrete Beams; Concrete T-Beams, T- and Double T-Sections	a, e, k and also i, j if sufficiently connected to act as a unit	$0.36 + \frac{S}{25.0}$	$0.2 + \frac{S}{12} - \left(\frac{S}{35}\right)^{2.0}$	$3.5 \leq S \leq 16.0$ $20 \leq L \leq 240$ $4.5 \leq t_s \leq 12.0$ $N_b \geq 4$
		Lever Rule	Lever Rule	$N_b = 3$

Table 12 – Distribution of Live Loads for Moment in Exterior Longitudinal Beam
(AASHTO LRFD *Bridge Design Specifications*, 2017)

Type of Superstructure	Applicable Cross-Section from Table 4.6.2.2.1-1	One Design Lane Loaded	Two or More Design Lanes Loaded	Range of Applicability
Concrete Deck, Filled Grid, Partially Filled Grid, or Unfilled Grid Deck Composite with Reinforced Concrete Slab on Steel or Concrete Beams; Concrete T-Beams, T- and Double T-Sections	a, e, k and also i, j if sufficiently connected to act as a unit	Lever Rule	$g = e g_{interior}$ $e = 0.77 + \frac{d_e}{9.1}$	$-1.0 \leq d_e \leq 5.5$
			use lesser of the values obtained from the equation above with $N_b = 3$ or the lever rule	$N_b = 3$

Table 13 – Distribution of Live Loads for Shear in Exterior Longitudinal Beam
(AASHTO LRFD *Bridge Design Specifications*, 2017)

Type of Superstructure	Applicable Cross-Section from Table 4.6.2.2.1-1	One Design Lane Loaded	Two or More Design Lanes Loaded	Range of Applicability
Concrete Deck, Filled Grid, Partially Filled Grid, or Unfilled Grid Deck Composite with Reinforced Concrete Slab on Steel or Concrete Beams; Concrete T-Beams, T- and Double T-Beams	a, e, k and also i, j if sufficiently connected to act as a unit	Lever Rule	$g = e \, g_{interior}$ $e = 0.6 + \frac{d_e}{10}$	$-1.0 \leq d_e \leq 5.5$
			Lever Rule	$N_b = 3$

The additional analysis is required for the exterior beam because of the existence of the diaphragm or cross-frame:

$$R = \frac{N_L}{N_b} + \frac{X_{ext} \sum_{N_b}^{N_L} e}{\sum x^2} \quad \text{Equation. 24}$$

where, R is reaction on exterior beam in terms of lanes, N_L is number of loaded lanes under consideration, e is eccentricity of a design truck or a design lane load from the center of gravity of the pattern of girders (ft), x is horizontal distance from the center of gravity of the pattern of girders to each girder (ft), X_{ext} is horizontal distance from the center of gravity of the pattern of girders to the exterior girder (ft), N_b is number of beams or girders.

For the target bridge to be load rated, all of the above GDFs were went through. Based on the inspection report, the bridge curb-to-curb width is 23 ft. Number of lanes to be considered is $23/12=1.9$, so that only one lane is considered. The distribution factors for the stringer is summarized in Table 14.

Table 14 – Summary of Girder Distribution Factors for Structure No. 020033G

	Moment (GDM)	Shear (GDF)
Interior Stringer	0.40	0.50
Exterior Stringer	0.36	0.36

4.4. Live Load Effects Using Finite Element Model

In this thesis, the finite element model (FEM) is proposed to get the live load effects. There are mainly two reasons for doing the FEM. The first one is with respect to the range of applicability of the AASHTO GDF equations. In the floorbeam system, the stringers directly support the deck and the stringers are in longitudinal directions so that the stringers are treated as girders, and AASHTO GDF equations can be applied in order to determine the live load effects on the stringer. However, the AASHTO GDF can only be applied when some certain criteria are satisfied. As shown in Table 10 to Table 13, there are ranges of applicability for each equation. For example, the moment distribution factor for interior girders can be applied only if:

- $3.5 \text{ ft} \leq \text{Spacing} \leq 16.0 \text{ ft}$
- $4.5 \text{ in} \leq \text{Slab thickness} \leq 12.0 \text{ in}$
- $20 \text{ ft} \leq \text{Span length} \leq 240 \text{ ft}$
- Number of girder ≥ 4
- $10,000 \leq K_g \leq 7,000,000$

As mentioned in the previous section, the AASHTO GDF equations target at the beam-slab bridge instead of the floorbeam system bridge. In the floorbeam system, the stringers are usually short and have small member sizes. Based on both steel truss bridge inventory and the bridge with no plan, the stringer length does not always satisfy the limitation for the girder length ($20 \text{ ft} \leq L \leq 240 \text{ ft}$), and the stiffness parameter K_g is found to be possibly less than $10,000 \text{ in}^4$ due to the small section. Sometimes the stringer spacing is also too narrow to satisfy applicability range. Thus, in the case that the stringers do not satisfy the applicability range of the AASHTO GDF equations, it is needed to find another way to obtain the live load effects. The FEM is accordingly proposed to find the live load effects.

Besides, as will show in the later chapter, the rating factors of the floorbeam is found to be relatively low compared with other structural elements. The possible reason could be attributed to the over-estimated live load effects on the floorbeam. According to the *AASHTO LRFD Bridge Design Specifications*, in the case that the transverse floorbeam does not directly support the bridge, then there is no need to calculate the distribution factors for the floorbeams. While doing the hand calculation, the live load applied to the floorbeam is herein shown in Figure 15. It is assumed that each stringer will transfer the ($GDF \times \text{total shear force caused by the truck}$). However, in reality, it is impossible for all the stringers to transfer that much load, especially for the stringers that is far from the truck. On account of the above-mentioned situation, the need for a FEM arises.

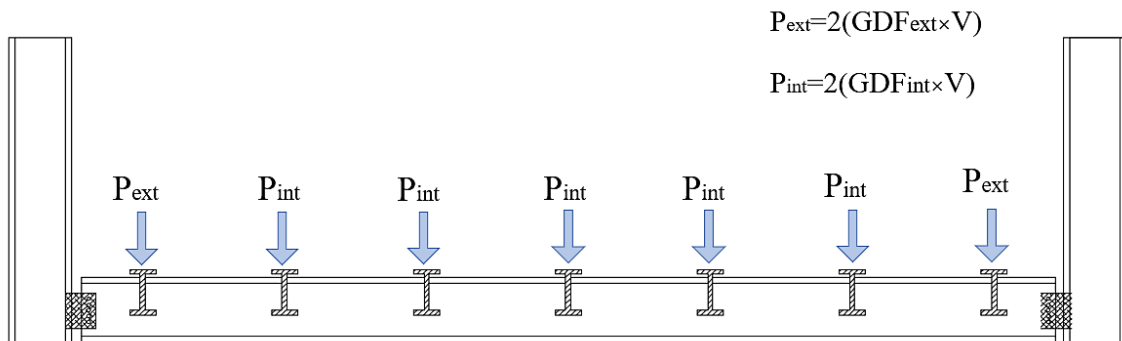
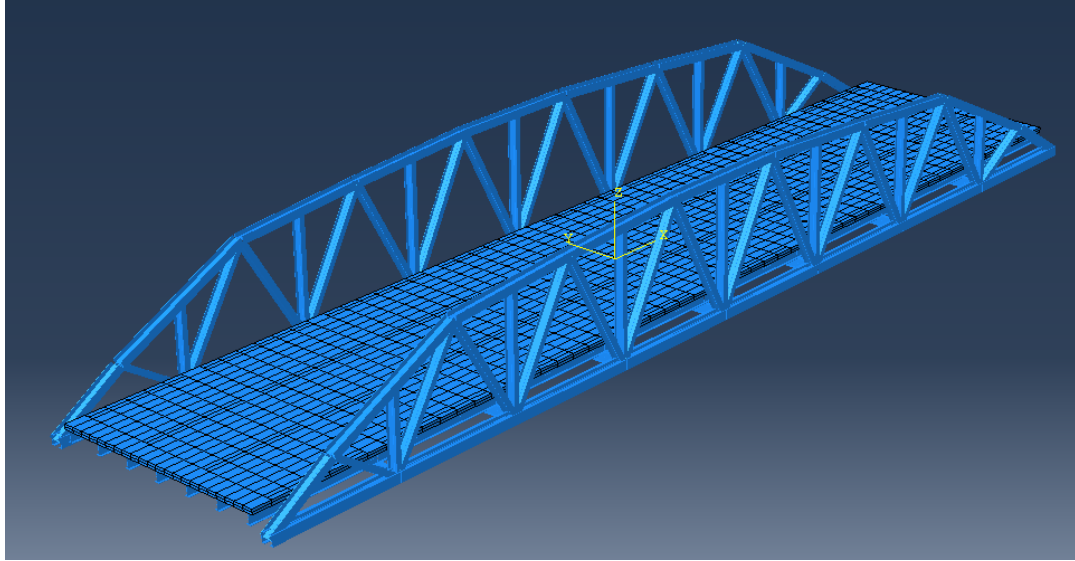
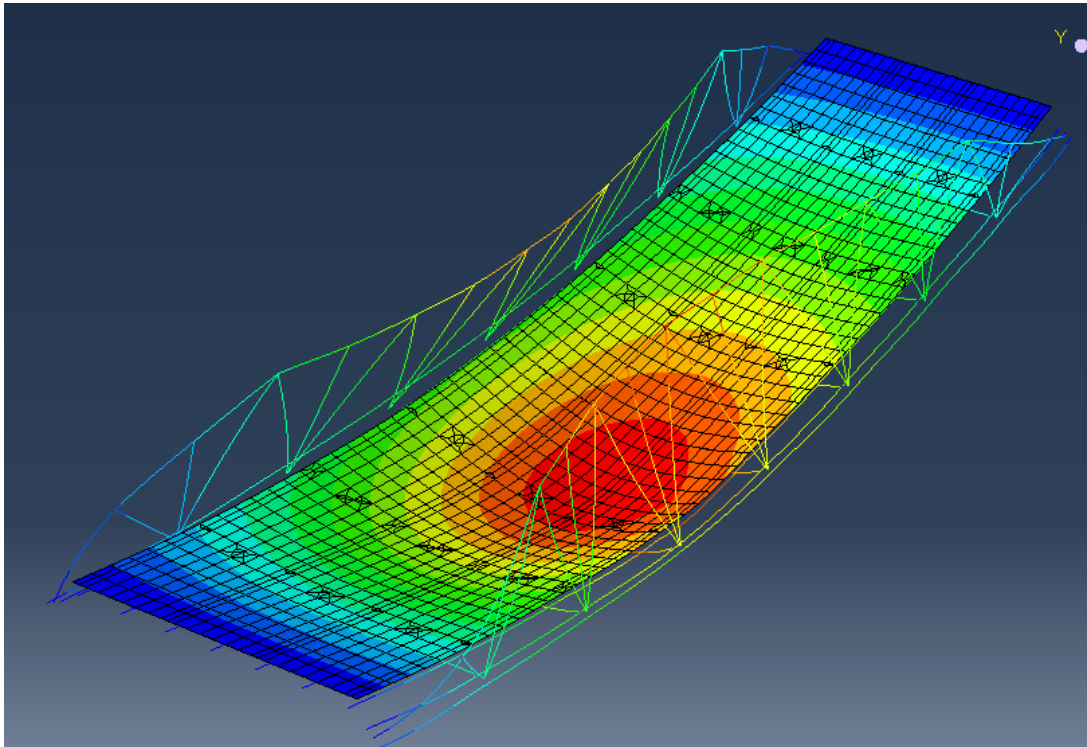


Figure 15. Cross-Section View of the Truss Bridge & Schematic Drawing of the Live Load Applied to the Floorbeam Based on Hand Calculation

The finite element model for the target bridge, SN 020033G, was then built by Abaqus as shown in Figure 16.



(a) General View of the FEM



(b) Simulation of Bridge Deformation under HL93 Load

Figure 16. Abaqus Model for the Bridge with No Plans (SN. 020033G)

In order to compare the live load effects by using hand calculation and using the finite element model, Table 15 and Table 16 list the live load effects by two different methods respectively. It is observed that the live load effects are significantly reduced by using FEM.

Table 15 – Hand Calculation Results- Live Load Effects on the Floorbeam

Live Load Effects	Design Load		Legal Load			Permit
	Tandem	Lane Load	Type 3	Type 3-3	Type 3S2	NJ Permit
Moment, kip-ft	423.91	42.69	381.13	315.41	383.75	643.28
Shear, kips	68.86	6.93	61.91	51.23	62.34	104.49
Stress, ksi	22.91	2.31	20.60	17.04	20.74	34.77

Table 16 – Finite Element Model Outputs- Live Load Effects on the Floorbeam

Live Load Effects	Design Load		Legal Load			Permit
	Tandem	Lane Load	Type 3	Type 3-3	Type 3S2	NJ Permit
Moment, kip-ft	131.54	63.27	217.38	215.53	223.30	635.11
Shear, kips	22.30	5.60	33.31	26.68	31.95	90.17
Stress, ksi	7.11	3.42	11.75	11.65	12.07	34.33

Chapter V

5. Analysis of Site-Specific Live Load Factor of Legal Load

5.1. Generalized Live Load Factors, γ_L for Routine Commercial Traffic

The AASHTO MBE provides the generalized live load factors for the Strength I limit state for routine commercial traffic, which are the AASHTO legal loads and State legal loads that have only minor variations from the AASHTO legal loads, on structures other than buried structures. The generalized live load factor, γ_L for routine commercial traffic provided by AASHTO MBE is listed in Table 17. These live load factors, involving the reliability analysis, were derived based upon a basis of the AASHTO LRFD Bridge Design with some modifications:

- The reliability index is 3.5 for the index level is 3.5, and the index is reduced to 2.5 for the operating (evaluation) level.
- The live load factor for LRFD considers 75-year truck traffic, and this period is reduced to 5-year for evaluation.
- In the LRFD, the multiple presence factors are based on the most extreme possible causes; in LRFR, the multiple presence factors herein are derived based on the most likely traffic condition.

Table 17 provides the live load factors that involve the above consideration. Reduced live load factors have been recommended because the original live load factors produced a higher reliability index than 2.5, which is the target reliability index for evaluation. Results of this study may be found in NCHRP Report 700 (Mlynarski et al., 2011).

Table 17 – Generalized Live Load Factors, γ_L for Routine Commercial Traffic

Traffic Volume (One Direction)	Load Factor
Unknown	1.45
$ADTT \geq 5,000$	1.45
$ADTT \leq 1,000$	1.30

5.2. Site- Specific Live Load Factors

5.2.1. Introduction and Motivation

In bridge, live loads exhibited a lot of uncertainties, so that the main purpose of the LRFR is to address the live load uncertainties. In general, LRFR directly uses the live load factors which is consistent with the AASHTO LRFD Specifications. These live load factors for design may be overly conservative for load rating and posting. The MBE Manual allows the site-specific live load factors that are developed by performing the statistical analysis of weigh-in-motion (WIM) data at or near the bridge site. The WIM system is widely used to determine the actual site survey of truck weight spectra and volume. WIM technology involves using axle sensors and other measurement systems which can detect the vehicle arrivals, determine the axle loads and gross vehicle weights, vehicle configurations, and the traveling speed. Based on the above-mentioned advantages of the WIM system, the WIM data can be utilized to provide a precise site-, route-, or region-specific load factors when refining LRFR load capacity calculations by collecting the truck traffic data at a specific site, along with a specific route, or around a specific region. Depending on the traffic weights and volumes, these load factors can be either higher or lower than the generalized live load factors listed in the MBE manual. The site-specific live load factor is also able to address the site-to-site variability of live load, and thus increase the accuracy

of the rating factors for a specific bridge. For the bridge that locates near the residential area, the average daily truck traffic (ADTT) and the truck weight and the corresponding live load factors are expected to be low; however, if the site observation shows the existence of overload, the live load factor may also increase rather than reduce. In this thesis, as described in the previous chapter, the target bridge to be load rated is located in a rural residential area and has very low ADTT on record. As a result, it could be possibly considered that the generalized live load factors may be higher than needed when load rating this bridge. The site-specific live load factors can also potentially improve network efficiency, especially in the case that the prescribed live load factors lead to the need for load posting.

In this thesis, on account of the low truck traffic volume on the target bridge and the big amount of the WIM systems in New Jersey, the site-specific live load factors for the legal load under Strength I limit state are investigated. Based on the inventory of the WIM system, there is no WIM station which is very close to the target bridge, the WIM stations that locate in the same county where the target bridge locates at are selected. The bridge with no plans locates at Bergen county. From the WIM system inventory in New Jersey, six (6) WIM systems, as shown in Table 18, were in use at Bergen County, so that the real truck traffic data from these six (6) WIM site are used to develop the site-specific live load factor.

Table 18 – WIM Site for Developing the Site-Specific Live Load Factors

Site ID	Route	Bound	Milepost	Municipality	County
000287	I-287	N&S	61.7	Franklin Lakes Boro	Bergen
000208	NJ-208	N&S	8.5	Franklin Lakes Boro	Bergen
0080DX	I-80	E	66.4	Hackensack City	Bergen
00017B	NJ-17	S	22.9	Ramsey Boro	Bergen
00003R	NJ-3	E&W	6.0	Rutherford Boro	Bergen
CO0821	CO-821	E&W	2.4	Ridgewood Village	Bergen

5.2.2. General Expressions for Site-Specific Live Load Factors

In NCHRP Report 454 (Moses, 2001), the Ontario truck data was used again to project the maximum loadings. It was found that for 5000 ADTT, the expected maximum loading in 2 years is 240 kips in 3S2 equivalent for two lanes or 120 kips per lane. In addition, the report also recommended the live load factor for Evaluation Manual as 1.80, which could represent the worst traffic category, namely 5000 ADTT. Starting with the nominal HL-93 load effects, which is 1.75, the adjusted live load factor for evaluation was composed of various considerations, including:

- From the study described in NCHRP Report 368 (Nowak, 1999), Nowak stated that the design live load factor of 1.6 is acceptable on the average, but the specification adopted 1.75 to be more conservative. The reduction factor of 0.91 (i.e., $1.6/1.75$) is considered when reducing the design load factor from 1.75 to 1.6.
- In the *AASHTO MBE* as well as the *AASHTO LRFD Bridge Design Specifications*, the inventory rating uses the live load factor of 1.75 for the HL93 nominal loading. In addition, an “operating” check with a live load factor of 1.35 is also prescribed. The reduction of live load factor from 1.75 to 1.35 reduces the safety index. The index for design is given as 3.5, whereas the index for evaluating the operating criteria is 2.5. Reduce the design target beta level from 3.5 to the corresponding

operating level of 2.5, resulting in a reduced load factor ratio of about 0.76 (i.e., 1.35 divided by 1.75).

- Compare the proposed live load factor for rating with the guide specification live load factor of 1.8, by considering that the guide used a target for beta corresponding to a love factor rating (LFR) of 2.3. This further reduces the live load factors by a factor of $1.90/1.95 = 0.92$.
- Reduce the live load factor to account for a 5-year instead of a 75-year, exposure.

Using Nowak's Projection (Nowak, 1999) of the expected maximum load effect for different durations, as shown in Table 19, produces a reduction of roughly 0.94.

The ratio of the two columns is about 0.94 on average.

Table 19 - Mean Maximum Moments for Simple Spans Decided by Corresponding New LRFD Moment (Nowak, 1999)

Span (ft)	M(LRFD) (k-ft)	1 day	2 weeks	1 month	2 months	6 months	1 year	5 years	50 years	75 years
10	88	0.88	1.02	1.07	1.12	1.18	1.25	1.33	1.50	1.50
20	232	0.90	0.98	1.02	1.06	1.10	1.14	1.21	1.30	1.30
30	397	0.95	1.04	1.08	1.12	1.15	1.19	1.26	1.35	1.35
40	578	1.02	1.11	1.14	1.17	1.21	1.23	1.28	1.35	1.35
50	826	1.00	1.08	1.12	1.15	1.18	1.22	1.25	1.33	1.33
60	1093	1.02	1.09	1.12	1.15	1.18	1.21	1.24	1.32	1.32
70	1376	1.02	1.08	1.12	1.15	1.18	1.21	1.25	1.31	1.31
80	1675	1.02	1.08	1.11	1.14	1.17	1.21	1.25	1.32	1.32
90	1990	1.02	1.08	1.11	1.14	1.16	1.20	1.24	1.31	1.31
100	2322	1.02	1.08	1.10	1.13	1.16	1.20	1.24	1.31	1.31
110	2670	1.02	1.07	1.10	1.12	1.15	1.19	1.24	1.31	1.31
120	3033	1.01	1.07	1.09	1.12	1.15	1.18	1.22	1.29	1.29
130	3413	1.00	1.06	1.09	1.11	1.13	1.16	1.20	1.27	1.27
140	3809	0.98	1.03	1.06	1.08	1.10	1.13	1.17	1.24	1.24
150	4220	0.98	1.03	1.06	1.07	1.09	1.12	1.16	1.23	1.23
160	4648	0.98	1.03	1.07	1.09	1.10	1.13	1.17	1.24	1.24
170	5092	0.99	1.03	1.07	1.09	1.11	1.13	1.18	1.24	1.24
180	5552	0.98	1.03	1.06	1.08	1.11	1.13	1.17	1.24	1.24
190	6028	0.97	1.02	1.06	1.08	1.10	1.13	1.17	1.24	1.24
200	6520	0.96	1.02	1.05	1.08	1.09	1.12	1.16	1.23	1.23

- Compare the nominal HL93 bending effects with those of the nominal AASHTO legal vehicles given in Table 20 to show an average ratio of 1.73.

Table 20 – Comparisons of the Simulated Mean Maximum Lane Moment, HL93, AASHTO Legal Vehicles and HS20 Load Models (Moses, 2001)

span FT.			M_{LRFD}			M_{HS20}	M_{LRFD}
	M_{LRFD}	M_{3S2}	M_{3S2}	M_{HS20}	M_{3S2}	M_{HS20}	M_{HS20}
40	588	324	1.82	450	1.39	1.31	
60	1093	618	1.77	807	1.31	1.35	
80	1675	974	1.72	1165	1.20	1.44	
100	2323	1332	1.74	1524	1.14	1.52	
120	3034	1690	1.80	1883	1.11	1.61	
			ave. = 1.77		= 1.23	= 1.45	

span FT.			M_{LRFD}	M_{75}	M_{HS20}
	M_{75}	M_{LEGAL}	M_{LEGAL}	M_{LEGAL}	M_{LEGAL}
40	783	350	1.68	2.24	1.29
60	1444	618	1.77	2.34	1.31
80	2202	974	1.72	2.26	1.20
100	3048	1343	1.73	2.27	1.14
120	3917	1743	1.74	2.25	1.08
			ave. = 1.73		1.20

M_{LRFD} —HL93 design bending moment

M_{LEGAL} —Maximum of three AASHTO legal vehicles (AASHTO,1994a)

M_{3S2} —3S2 bending moment

M_{HS20} —Previous AASHTO load model (AASHTO, 1998)

M_{75} —Simulated mean maximum bending moment from Nowak Table B-11 (Nowak,1999).

Balancing all the considerations shown above, the final live load factors were derived shown in Equation 25. The value is finally recommended for the Evaluation Manual is 1.80 for the worst traffic category, namely 5000 ADTT.

$$1.75HL-93 = 1.75 \times 0.91 \times 0.76 \times 0.94 \times 1.73 \times 0.92 \times 3S2 = 1.81 \times 3S2 \quad \text{Equation 25}$$

Combining the live load factor 1.8 with the expected maximum live load, which is 120 kips for single-lane and 240 kips for double-lane (in 3S2 equivalents), the general expression of the evaluation live load factor for any specific application are shown in Equation 26 and Equation 27.

$$\gamma_{L, one-lane} = 1.8 \times \frac{LL_{\max, one-lane}}{120 \text{ kips}} \quad \text{Equation 26}$$

$$\gamma_{L, two-lane} = 1.8 \times \frac{LL_{\max, two-lane}}{240 \text{ kips}} \quad \text{Equation 27}$$

These two equations were adopted by MBE with small changes. In MBE, while using these equations, the load effects from the 120-kip 3S2 truck are considered rather than the weight. Thus, the equations adopted by MBE for calculating the site-specific legal load factors for the Strength I limit state become *Equation 28* and *Equation 29*.

For one lane loading case:

$$\gamma_{L1} = \left[\frac{L_{\max 1}}{LE_1} \right] 1.8 > 1.8 \quad \text{Equation 28}$$

For two or more loading case:

$$\gamma_{L2} = \left[\frac{L_{\max 2}}{LE_2} \right] 1.8 > 1.3 \quad \text{Equation 29}$$

Where:

$L_{\max 1}$ = Maximum single-lane load effect expected over a 5-year period

$L_{\max 2}$ = Maximum two or more lanes load effect expected over a 5-year period

LE_1 = Maximum load effect from one 120 K, 3S2 truck side by side

LE_2 = Maximum load effect from two 120 K, 3S2 trucks side by side

It is noticeable that MBE sets the lower bound limits as 1.8 for one-lane loaded case and 1.3 for the two-lane loaded case. The reason for these limits is because NCHRP Report 454 (Moses, 2001) claims that the lower limit of 1.8 for the one-lane bridge is arbitrarily placed on the one-lane factor based on the experience with WIM data. This report also provides the lower bound of 1.30 which is less than the live load factor of 1.4 for 100 ADTT at that time. It was stated that the smaller factor is reasonable because the direct use of a site's

WIM weight database will reduce the uncertainties in a predictable maximum loading event compared with the use of the Ontario data presented by Nowak.

For the purpose of deriving the live load factors for the legal load, the legal trucks should be firstly screened out from the traffic stream. The filter criteria are based on the NCHRP Report 575 (Sivakumar et al., 2007). There are four basic federal weight limits:

1. 22,400 lbs for single axles as per NJDOT weight limits
2. 34,000 lbs for tandem axles, where the tandem is defined as two or more consecutive axles more than 40 in. but no more than 96 in. apart
3. A maximum GVW of 80,000 lbs, and
4. Application of the Federal Bridge Formula (FBF) B for each axle group up to the maximum GVW. FBF B is given as follow:

$$W = 500 \left[\frac{LN}{N-1} + 12N + 36 \right] \quad \text{Equation 30}$$

where, W = the maximum weight in pounds that can be carried on a group of two or more axles to the nearest 500 lbs,

L = the distance in feet between the outer axles of any two or more consecutive axles, and

N = the number of axles being considered.

5.3. Estimation of the Maximum Load Effect, L_{\max}

As discussed in the last section, *AASHTO MBE* provides a way to calculate the site-specific live load effects according to the NCHRP Report 454 (Moses, 2011). In order to calculate the live load factor, γ_L , the maximum load effect expected over a 5-year period will firstly

need to be determined. The most straightforward method is to directly obtain the 5-year truck traffic data from the WIM system, and then the maximum load effects that appeared in the 5 years period can be determined. However, this method requires a lot of data processing, and some of the WIM stations are not old enough to provide the data for 5 years. In these cases, the maximum load effects will need to be estimated based on the currently available data. The estimation of the maximum load effect, L_{\max} , expected over a 5-year bridge evaluable period can be executed through a variety of methods. In this thesis, two methods for estimating the maximum live load effects are investigated and implemented.

5.3.1. Gumbel Distribution

One of the methods to estimate the maximum live load factor, according to the study performed in NCHRP Report 683 (Sivakumar et al., 2011), is based on the assumption that the tail end of the histogram of the maximum load effect over a given return period approaches a Gumbel distribution as the return period increases. This method is also adopted by AASHTO MBE.

In order to apply this assumption, WIM data should be collected during a sufficiently long period in order to catch the representative tile-end truck weight data. The method first assumes the tile end of the live load effects is Normal distribution, and then the closed-form equations are applied to transfer the Normal distribution to the Gumbel distribution. The Normal distribution, based on the experience of the WIM data, can usually be found at the top 5% live load effects.

The maximum live load effects can be estimated based on the following procedure:

- Obtain the live load effects for a suite of simple and continuous spans by using influence line.
- Assemble the load effects in the increasing order.
- Calculate the cumulative distribution function (CDF) and the standard deviate for each type of load effect (positive moment, negative moment, and shear)
- Plot the upper five percent of the data of the normal deviate versus the load effect.
- Finding the best-fit regression line of the above plot, the slope, m , and intercept, n , of the regression line, would provide the statistics for the normal distribution that best fits the tail end of the distribution.
- The mean of Normal that best fits the tail end of the distribution is calculated using Equation 31.

$$\mu_{event} = -n / m \quad \text{Equation 31}$$

- The standard deviation of the best fit normal distribution is calculated using Equation 32.

$$\sigma_{event} = 1 / m \quad \text{Equation 32}$$

- Let n_{day} = total number of trucks per day
- For 5 years: $N = n_{day} \times 365 \times 5$
- The most probable value, u_N , for the Gumbel distribution that models the maximum value in 5 years L_{max} is given by Equation 33.

$$u_N = \mu_{event} + \sigma_{event} \times \left[\sqrt{2 \ln(N)} - \frac{\ln(\ln(N)) + \ln(4\pi)}{2\sqrt{2 \ln(N)}} \right] \quad \text{Equation 33}$$

- The dispersion coefficient for the Gumbel distribution that models the maximum load effect L_{max} is given by Equation 34 and Equation 35.

$$\alpha_N = \frac{\sqrt{2\ln(N)}}{s_{event}} \quad \text{Equation 34}$$

- The mean value of Lmax is given as Equation 35.

$$L_{\max} = u_{\max} = u_{event} + \frac{0.577216}{\alpha_N} \quad \text{Equation 35}$$

The WIM data processing and the calculations of the maximum load effect will be illustrated in the later section.

5.3.2. Normal Distribution

Another method is developed by NCHRP Report 368 (Nowak, 1999). This method directly assumes that the tail end of the maximum load effect over a given return period approaches a Normal distribution, and then further extrapolate the data for the 5-year period based on the Normal distribution. The maximum live load effects can be estimated based on the following procedure:

- Obtain the live load effects for a suite of simple and continuous spans by using influence line.
- Arrange the live load effect, x , in an increasing order (x_1 is the smallest and x_n is the largest value)
- The probability, p , of the cumulative distribution function (CDF), is calculated by *Equation 36*.

$$p_i = \frac{i}{X + 1} \quad \text{Equation 36}$$

where, X = population size

- The inverse standard normal distribution scale, z , can be transformed from the probability by using Equation 37.

$$z = \Phi^{-1}[p] \quad \text{Equation 37}$$

where Φ^{-1} = inverse of the standard normal distribution function

- A plot is made of the inverse standard normal values versus the bias ratio, which is the live load effect/3S2 truck load effect. It is assumed that the upper five percent of the CDF approaches a Normal distribution function so that the best-fit regression line is made for the upper five percent of the live load effect/3S2 truck load effect.
- Let n_{day} = total number of trucks per day
- For 5 years: $N = n_{day} \times 365 \times 5$
- The corresponding probability for N is $p_N = \frac{N}{N+1}$, and the z value is accordingly

$z = \Phi^{-1}[p_N]$ so that the available data can be extrapolated to determine the maximum expected load effects for the 5-year period.

The reason for the extrapolation is because there are a lot of uncertainties involved in the analysis due to limitations and biases in the survey data. Even though there are ten thousand truck data available, it is very small compared to the actual number of heavy vehicles in a 5-year period. Thus, it is important to extrapolate the short-term data to estimate the future maximum live load effect.

5.4. WIM Data Processing Demonstration

5.4.1. Step One: Read Data

In this study, the live load effect is considered in terms of a positive moment on the simple span, the negative moment on continuous spans. The shear is not considered because the shear is usually less critical than the moment. A suite of simple spans and two equal continuous spans with the span lengths from 20 ft to 200 ft are considered. This demo uses the WIM data collected in June 2016 at the WIM site CO082116. By applying the four basic federal weight limits, 4493 legal trucks were screened out from 4703 trucks.

5.4.2. Step Two: Hypothesis Testing

After screening out the legal trucks, corresponding positive moments and negative moment of all the span lengths caused by each legal truck were calculated by using MATLAB.

Since the demo only uses a 1-month dataset, the maximum live load effects in the 5-year period will need to be estimated. As mentioned in Section 5.3, two ways to estimate L_{\max} are proposed in this study: the first one assumes a Gumbel distribution for the tail end of the live load effects, whereas the other one assumes a Normal distribution for the tail end of the live load effects. With the intent to determine the better fit distribution, hypothesis testing is required to statistically verify whether the assumption is true. A program, called EasyFit, was used to do the hypothesis testing in this study. This program is able to verify the goodness of fit for 61 types of distributions, among which the Gumbel distribution and the Normal distribution are also in the lists. To use this program, one or more variables should be input into the, and then the program will automatically analysis the goodness of fit of each distribution, and further rank the distributions from the best-fit to the least-fit.

The live load effects are herein input into the program, and the ranks of the Gumbel distribution and the Normal distribution is compared. It is observed that both the positive moment and the negative moment are better correlated to the Gumbel distribution. Thus, it is suggested to use Gumbel distribution for estimating the L_{max} .

5.4.3. Step Three: Estimation of L_{max} and γ_L

Although the hypothesis testing shows the Gumbel distribution is better fitted with the tail end of the live load effects, both methods are implemented in order to investigate the difference between the two methods. The first method assumes that the tail end of the histogram approaches a Gumbel distribution for a sufficiently long period of time. After obtaining the live load effects, which are positive moments and negative moments in this study, a plot is made of normal deviate versus load effect. For example, Figure 17 plots the curve for a simple span with span length of 60 ft, 80 ft, 120 ft, and 200 ft. The best-fit regression line for the upper 5% load effects are generated as shown below.

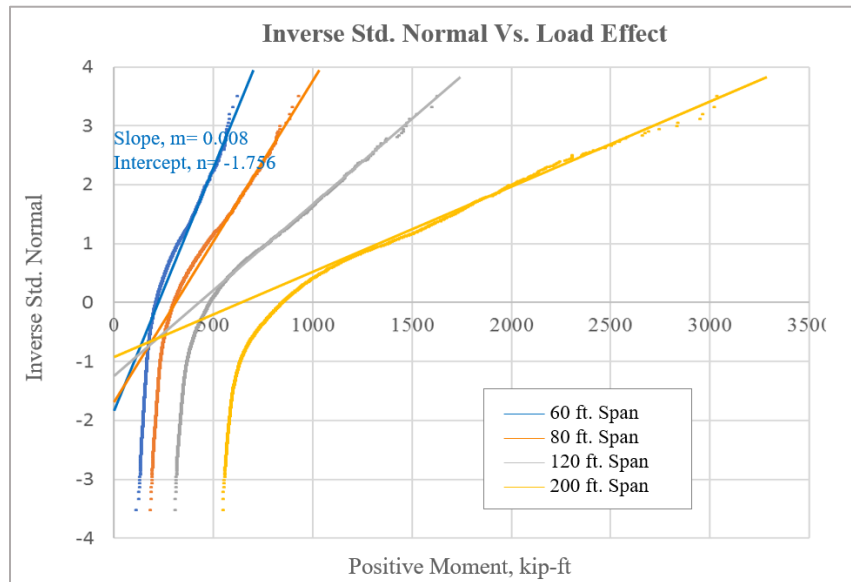


Figure 17. Demonstration of Estimating L_{max} assuming Gumbel Distribution

For the purpose of demonstration, the 60 ft span data are analyzed step by step. The calculations of the site-specific live load factor are as follow:

- The regression line has the slope $m=0.008$ and intercept $n=1.756$
- The mean of Normal that best fits the tail end of the distribution:

$$\mu_{event} = -n / m = 215.5$$

- The standard deviation of the best fit Normal:

$$\sigma_{event} = 1 / m = 122.8$$

- $n_{day} = \text{number of legal truck per day} = 157$

$$N = \frac{n_{day} \times 1000}{\text{Actual ADTT}} \times 365 \times 5 = 1,913,143$$

- For 5 years:
- The most probable value for the Gumbel distribution that models the maximum value in 5 years:

$$\mu_N = \mu_{event} + \sigma_{event} \left[\sqrt{2 \ln(N)} - \frac{\ln(\ln(N) + \ln(4\pi))}{2\sqrt{2 \ln(N)}} \right] = 814.4$$

- The dispersion coefficient for the Gumbel distribution that models the maximum load effect L_{max} :

$$\alpha_N = \frac{\sqrt{2 \ln(N)}}{\sigma_{event}} = 0.0437$$

- The mean value of L_{max} is given as:

$$L_{max} = \mu_N + \frac{0.577216}{\alpha_N} = 826.6$$

- The site-specific live load factor is:

$$\gamma_L = 1.8 \times \frac{L_{max}}{LE_1} = 1.8 \times 0.79 = 1.42$$

The second methods to estimate the maximum live load factor assumes that the upper tile of the live load effects follows the Normal distribution. Using the same data set as the first method just used, a plot is made of the inverse standard normal versus nominalized moment (Moment/3S2 Truck Moment). Same as Method 1, the moment on the simple spans with a span length of 60 ft, 80ft, 120 ft, and 200 ft are plotted in Figure 18.

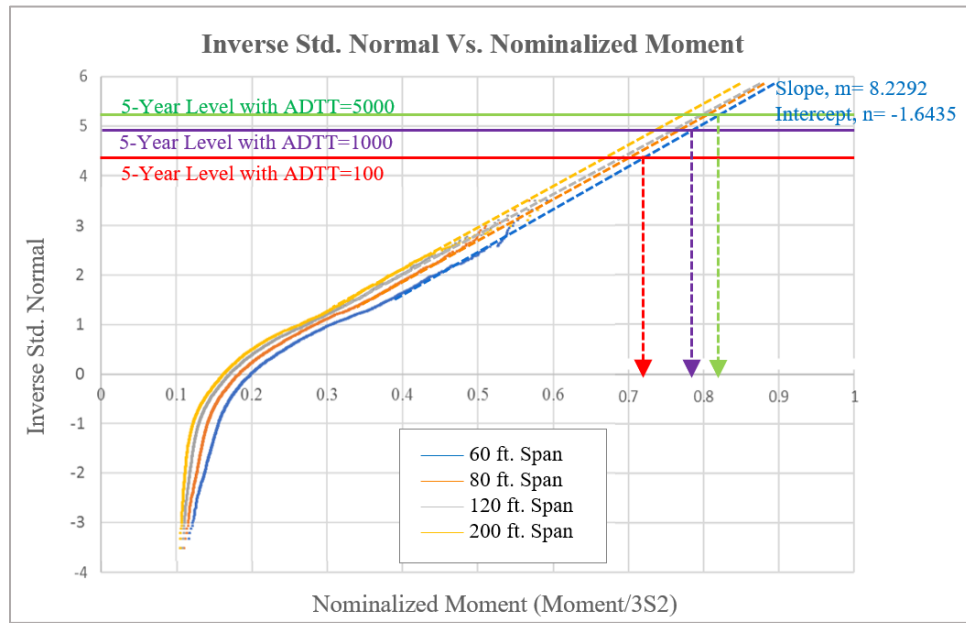


Figure 18. Demonstration of Estimating L_{\max} assuming Normal Distribution

For demonstration and comparison, the 60 ft span data are analyzed step by step. The calculations of the site-specific live load factor are as follow:

- The best-fit regression line for the upper 5% live load effects has the expression of:

$$\Phi^{-1}\left(\frac{N_{5\text{-year}}}{N_{5\text{-year}} + 1}\right) = 8.23 \times \text{Nomalized Moment}_{5\text{-year}} - 1.6435$$

- n_{day} = number of legal truck per day = 157

$$N = \frac{n_{day} \times 1000}{Actual\ ADTT} \times 365 \times 5 = 1,913,143$$

- For 5 years:
- The inverse standard normal value for N is:

$$\Phi^{-1}\left(\frac{N_{5-year}}{N_{5-year} + 1}\right) = \Phi^{-1}\left(\frac{1,913,143}{1,913,144}\right) = 4.88$$

- Plug the inverse standard normal into the regression line:

$$\Phi^{-1}\left(\frac{N_{5-year}}{N_{5-year} + 1}\right) = 8.23 \times Normalized\ Moment_{5-year} - 1.6435$$

- The maximum normalized moment in 5 years is estimated as:

$$Normalized\ Moment_{5-year} = \frac{4.88 + 1.6435}{8.23} = 0.79$$

- The site-specific live load factor is calculated as:

$$\gamma_L = 1.8 \times \frac{L_{max}}{LE_1} = 1.8 \times 0.79 = 1.42$$

By repeating the above procedures for all the other spans and different ADTTs, the bias ratio shown in Table 21 can be obtained.

Table 21 – Bias Ratio for Simple Span (WIM Site CO082116)

Bias Ratio (CO082116)		ADTT \leq 100	100 < ADTT \leq 1000	1000 < ADTT \leq 5000
20 ft	Gumbel Dist.	0.81	0.86	0.90
	Normal Dist.	0.79	0.85	0.88
40 ft	Gumbel Dist.	0.81	0.87	0.91
	Normal Dist.	0.72	0.85	0.89
60 ft	Gumbel Dist.	0.73	0.79	0.82
	Normal Dist.	0.72	0.79	0.81
80 ft	Gumbel Dist.	0.69	0.74	0.78
	Normal Dist.	0.68	0.73	0.76
100 ft	Gumbel Dist.	0.69	0.74	0.78
	Normal Dist.	0.67	0.73	0.76
120 ft	Gumbel Dist.	0.76	0.76	0.79
	Normal Dist.	0.68	0.74	0.78
140 ft	Gumbel Dist.	0.71	0.77	0.80
	Normal Dist.	0.69	0.75	0.79
160 ft	Gumbel Dist.	0.72	0.78	0.82
	Normal Dist.	0.70	0.76	0.80
180 ft	Gumbel Dist.	0.72	0.78	0.82
	Normal Dist.	0.70	0.77	0.81
200 ft	Gumbel Dist.	0.73	0.79	0.83
	Normal Dist.	0.71	0.77	0.82

For the above table, it is observed that the two methods give very close results. In order to better compare the two methods, the percent differences are calculated for the bias ratio of all the WIM sites and all the span lengths.

Table 22 and Table 23 show the percent difference for the positive moment and negative moment respectively.

Table 22 – Percent Difference of Gumbel Distribution vs. Normal Distribution – Positive Moment

% Difference		20 ft	40 ft	60 ft	80 ft	100 ft	120 ft	140 ft	160 ft	180 ft	200 ft
00003R	ADTT=100	1.89	2.07	2.12	2.14	2.23	2.31	2.37	2.43	2.46	2.49
	ADTT=1000	1.60	1.74	1.79	1.81	1.86	1.95	1.99	2.03	2.05	2.08
	ADTT=5000	1.46	1.58	1.61	1.63	1.69	1.74	1.78	1.82	1.85	1.87
00017B	ADTT=100	1.12	1.31	1.39	1.45	1.28	1.21	1.19	1.19	1.18	1.17
	ADTT=1000	0.97	1.13	1.21	1.25	1.11	1.06	1.05	1.04	1.03	1.02
	ADTT=5000	0.89	1.04	1.10	1.14	1.01	0.98	0.95	0.94	0.94	0.94
000287	ADTT=100	0.78	1.00	1.07	1.35	1.10	0.97	0.90	0.86	0.84	0.84
	ADTT=1000	0.68	0.88	0.94	1.17	0.97	0.86	0.80	0.76	0.74	0.74
	ADTT=5000	0.63	0.81	0.85	1.07	0.88	0.79	0.74	0.70	0.70	0.69
CO082116	ADTT=100	1.89	2.07	2.12	2.14	2.23	2.31	2.37	2.43	2.46	2.49
	ADTT=1000	1.60	1.74	1.79	1.81	1.86	1.95	1.99	2.03	2.05	2.08
	ADTT=5000	1.46	1.58	1.61	1.63	1.69	1.74	1.78	1.82	1.85	1.87
000208	ADTT=100	1.14	1.33	1.45	1.57	1.46	1.42	1.39	1.38	1.38	1.38
	ADTT=1000	0.98	1.16	1.25	1.35	1.26	1.21	1.19	1.18	1.20	1.20
	ADTT=5000	0.90	1.06	1.14	1.22	1.14	1.11	1.09	1.08	1.08	1.09
0080DX	ADTT=100	0.67	0.93	0.91	1.14	0.92	0.78	0.74	0.70	0.68	0.67
	ADTT=1000	0.60	0.83	0.80	1.00	0.80	0.70	0.64	0.62	0.62	0.60
	ADTT=5000	0.56	0.76	0.74	0.92	0.74	0.64	0.59	0.58	0.56	0.56

Table 23– Percent Difference of Gumbel Distribution vs. Normal Distribution – Negative Moment

% Difference		20 ft	40 ft	60 ft	80 ft	100 ft	120 ft	140 ft	160 ft	180 ft	200 ft
00003R	ADTT=100	2.25	1.98	1.84	1.73	1.78	1.78	1.80	1.80	1.81	1.82
	ADTT=1000	1.88	1.67	1.55	1.48	1.51	1.52	1.53	1.53	1.54	1.54
	ADTT=5000	1.69	1.52	1.41	1.35	1.37	1.38	1.39	1.40	1.40	1.40
00017B	ADTT=100	1.49	1.30	1.24	1.30	1.22	1.19	1.17	1.17	1.16	1.18
	ADTT=1000	1.29	1.11	1.07	1.11	1.06	1.03	1.03	1.02	1.02	1.02
	ADTT=5000	1.16	1.02	0.98	1.02	0.98	0.94	0.92	0.93	0.94	0.94
000287	ADTT=100	1.16	0.97	0.91	0.98	0.95	0.88	0.84	0.84	0.83	0.83
	ADTT=1000	1.02	0.85	0.80	0.85	0.84	0.77	0.76	0.74	0.73	0.72
	ADTT=5000	0.94	0.78	0.74	0.78	0.77	0.71	0.70	0.68	0.67	0.67
CO082116	ADTT=100	2.24	2.75	2.82	2.49	2.44	2.53	2.60	2.63	2.66	2.69
	ADTT=1000	1.89	2.27	2.33	2.08	2.04	2.10	2.15	2.18	2.20	2.22
	ADTT=5000	1.70	2.02	2.07	1.86	1.82	1.89	1.93	1.95	1.96	1.97
000208	ADTT=100	1.58	1.46	1.47	1.54	1.39	1.38	1.37	1.38	1.37	1.39
	ADTT=1000	1.35	1.27	1.26	1.32	1.20	1.18	1.19	1.19	1.20	1.20
	ADTT=5000	1.23	1.15	1.15	1.21	1.10	1.08	1.08	1.09	1.09	1.09
0080DX	ADTT=100	0.95	0.81	0.65	0.72	0.78	0.70	0.65	0.65	0.64	0.64
	ADTT=1000	0.84	0.73	0.59	0.65	0.68	0.62	0.58	0.57	0.58	0.58
	ADTT=5000	0.76	0.66	0.55	0.60	0.62	0.58	0.56	0.54	0.53	0.53

5.5. Proposed Live Load Factor for the Bridge with No Plan

From Table 22 and Table 23, it is noticed that the bias ratio calculated by the two methods are very close to each other. However, as mentioned before, according to the hypothesis testing, the Gumbel distribution is better fitted with the upper tile of the live load effects, so that the live load factors are calculated based on the Gumbel distribution. According to AASHTO MBE, the site-specific live load factors should address both the one-lane loading case and two-lane loading case. Nowak stated that for a two-lane bridge, the maximum 75-year live load effect is caused by two side-by-side trucks, each representing the maximum two-month vehicle. The two-lane loading case should involve using the multiple presences

to represent the case that two trucks are traveling side-by-side on the bridge, and should also involve the distribution of the truck load to the girders. However, due to the lack of accuracy of the WIM data, the multiple presence of the trucks (two-lane loading case) cannot be captured. In order to predict the maximum load effect on the two-lane bridge, an assumption is made in accordance with NCHRP Report 368 (Nowak, 1999): the 2-month maximum truck weight is 0.85 times the single lane expected maximum life-time load effect acting in each lane. As a result, Equation 29 becomes:

$$\gamma_{L2} = \left[\frac{L_{\max 2}}{LE_2} \right] 1.8 = \left[\frac{2 \times (0.85 L_{\max 1})}{2 \times LE_1} \right] 1.8 = 0.85 \gamma_{L1} \quad \text{Equation 38}$$

Recalling that there are 6 WIM sites in the county, the site-specific live load factors shall incorporate all of them. Each site can come up with a maximum live load factor, and the final rating factors are taken as the mean value of the maximum live load factor from each site. The site-specific live load factors Table 24 shows the site-specific live load factors proposed for this study, including both one-lane loading case and two-lane loading case. NCHRP Report 454 (Moses, 2001) stated that single-lane live load factors for legal load ratings are only necessary for situations where the bridge contains a single traffic lane. In this study, since the target bridge is a two-way traffic bridge, the live load factor for two-lane loading case is considered.

Table 24 – Proposed Site-Specific Live Load Factor, γ_L

Traffic Volume (One Direction)	Site-Specific $\gamma_{L(1\text{-lane})}$	Site-Specific $\gamma_{L(2\text{-lane})}$
$ADTT \leq 100$	1.58	1.34
$100 < ADTT \leq 1000$	1.67	1.42
$1000 < ADTT \leq 5000$	1.73	1.47

Chapter VI

6. Load Rating Results

6.1. Load Rating Results using Clustering Methodology

Recalling the proposed procedures for load rating the steel truss bridge with no plans, the unknown bridge sections were estimated based on the similar bridges in Chapter 3. In this section, the load rating will be performed based on the estimated sections. From Table 25 to Table 30, the rating factors based on the estimated section for the stringer, floorbeam, and truss members are presented.

Table 25 - Interior Stringer Rating Factors Based on Clustering Methodology

Limit State		Design Load		Legal Load			Legal Load
		Inv.	Op.	Type 3	Type 3-3	NJ 3S2	NJ-Permit
Strength I	Flexure	1.49	1.93	3.18	3.87	3.19	-
	Shear	2.45	3.18	3.49	4.22	3.47	-
Strength II	Flexure	-	-	-	-	-	2.33
	Shear	-	-	-	-	-	3.81
Service II		2.31	3.00	3.66	4.46	3.67	2.09

Table 26 - Exterior Stringer Rating Factors Based on Clustering Methodology

Limit State		Design Load		Legal Load			Legal Load
		Inv.	Op.	Type 3	Type 3-3	NJ 3S2	NJ-Permit
Strength I	Flexure	1.78	2.31	3.80	4.62	4.73	-
	Shear	4.88	6.33	4.94	5.97	6.09	-
Strength II	Flexure	-	-	-	-	-	2.46
	Shear	-	-	-	-	-	7.59
Service II		2.83	3.67	4.49	5.46	5.58	2.56

Table 27 - Floorbeam Rating Factors Based on Clustering Methodology

Limit State		Design Load		Legal Load			Legal Load
		Inv.	Op.	Type 3	Type 3-3	NJ 3S2	NJ-Permit
Strength I	Flexure	0.63	0.81	1.35	1.63	1.34	-
	Shear	1.66	2.16	3.56	4.30	3.54	-
Strength II	Flexure	-	-	-	-	-	0.90
	Shear	-	-	-	-	-	2.39
Service II		0.80	1.04	1.27	1.54	1.26	0.75

Table 28 – Top Chord Rating Factors Based on Clustering Methodology

Limit State		Design Load		Legal Load			Legal Load
		Inv.	Op.	Type 3	Type 3-3	NJ 3S2	NJ-Permit
Strength I	Axial	0.54	0.82	1.76	1.40	1.29	-
Strength II	Axial	-	-	-	-	-	0.62

Table 29 – Bottom Chord Rating Factors Based on Clustering Methodology

Limit State		Design Load		Legal Load			Legal Load
		Inv.	Op.	Type 3	Type 3-3	NJ 3S2	NJ-Permit
Strength I	Axial	0.54	0.70	1.33	1.04	0.96	-
Strength II	Axial	-	-	-	-	-	0.45

Table 30 – Diagonal Rating Factors Based on Clustering Methodology

Limit State		Design Load		Legal Load			Legal Load
		Inv.	Op.	Type 3	Type 3-3	NJ 3S2	NJ-Permit
Strength I	Axial	0.83	1.07	2.19	1.75	1.61	-
Strength II	Axial	-	-	-	-	-	0.75

6.2. Load Rating Results using Field Investigation

By taking advantage of the bridge location, the bridge was investigated in detail on site.

All of the structural elements were measured so that the member sizes are known at the end. In order to verify the clustering results as well as to improve the accuracy of the rating factors, the bridge is rated by using the actual member sizes. The rating factors of each structural elements are shown from Table 31 to Table 36.

Table 31 - Interior Stringer Rating Factors Based on Field Inspection

Limit State		Design Load		Legal Load			Legal Load
		Inv.	Op.	Type 3	Type 3-3	NJ 3S2	NJ-Permit
Strength I	Flexure	1.49 2.10	1.93 2.72	3.18 4.48	3.87 5.45	3.19 4.49	-
	Shear	2.45 2.83	3.18 3.78	3.49 4.03	4.22 4.87	3.47 4.00	-
Strength II	Flexure	- -	- -	- -	- -	- -	2.33 3.23
	Shear	- -	- -	- -	- -	- -	3.81 4.39
Service II		2.31 2.69	3.00 3.50	3.66 4.27	4.46 5.20	3.67 4.28	2.09 2.44

Table 32 - Exterior Stringer Rating Factors Based on Field Inspection

Limit State		Design Load		Legal Load			Legal Load
		Inv.	Op.	Type 3	Type 3-3	NJ 3S2	NJ-Permit
Strength I	Flexure	1.78 2.33	2.31 3.02	3.80 4.98	4.62 6.06	4.73 6.20	- -
	Shear	4.88 5.63	6.33 7.29	4.94 5.69	5.97 6.88	6.09 7.02	- -
Strength II	Flexure	- -	- -	- -	- -	- -	2.46 3.22
	Shear	- -	- -	- -	- -	- -	7.59 8.74
Service II		2.83 3.30	3.67 4.28	4.49 5.23	5.46 6.36	5.58 6.51	2.56 2.99

Table 33 – Floorbeam Rating Factors Based on Field Inspection

Limit State		Design Load		Legal Load			Legal Load
		Inv.	Op.	Type 3	Type 3-3	NJ 3S2	NJ-Permit
Strength I	Flexure	0.63	0.81	1.35	1.63	1.34	-
		0.63	0.81	1.34	1.62	1.33	-
	Shear	1.66	2.16	3.56	4.30	3.54	-
		1.66	2.15	3.56	4.30	3.53	-
Strength II	Flexure	-	-	-	-	-	0.90
		-	-	-	-	-	0.90
	Shear	-	-	-	-	-	2.39
		-	-	-	-	-	2.38
Service II		0.80	1.04	1.27	1.54	1.26	0.75
		1.66	2.15	3.56	4.30	3.53	0.75

Table 34 – Top Chord Rating Factors Based on Field Inspection

Limit State		Design Load		Legal Load			Legal Load
		Inv.	Op.	Type 3	Type 3-3	NJ 3S2	NJ-Permit
Strength I	Axial	0.54	0.82	1.76	1.40	1.29	-
		0.72	1.09	2.36	1.87	1.73	-
Strength II	Axial	-	-	-	-	-	0.62
		-	-	-	-	-	0.82

Table 35 – Bottom Chord Rating Factors Based on Field Inspection

Limit State		Design Load		Legal Load			Legal Load
		Inv.	Op.	Type 3	Type 3-3	NJ 3S2	NJ-Permit
Strength I	Axial	0.54	0.70	1.33	1.04	0.96	-
		1.90	2.46	4.72	3.66	3.40	-
Strength II	Axial	-	-	-	-	-	0.45
		-	-	-	-	-	1.34

Table 36 – Diagonal Rating Factors Based on Field Inspection

Limit State		Design Load		Legal Load			Legal Load
		Inv.	Op.	Type 3	Type 3-3	NJ 3S2	NJ-Permit
Strength I	Axial	0.83	1.07	2.19	1.75	1.61	-
		2.05	2.66	5.42	4.34	4.00	-
Strength II	Axial	-	-	-	-	-	0.75
		-	-	-	-	-	1.86

It is observed that for stringers, the clustering method provides reasonably smaller rating factors compared with the field inspection because when estimating the unknown member sizes, the conservative sections are chosen from the bridge cluster. Regarding the floorbeam, the clustering method provides an exact same section size as the actual size, leading to the same rating factors. However, the rating factors of truss members based on the clustering method are much smaller than the actual value. This result is in accordance with the expectation, because, as mentioned in Chapter 3, while selecting the reference bridge from the bridge cluster, the selected bridge has a much shorter span length than the target bridge. Besides, the target bridge has a sidewalk which is supported by the truss, whereas the reference bridge does not have a sidewalk.

6.3. Refinement of the Design Load Rating Using FEM

Based on the rating factors by using the field inspection results, it is observed that the floorbeam is the least rated elements. It is important to improve the rating factors of these two members. Thus, this section focuses on refining the rating factors of the floorbeam. The rating factors of the floorbeam based on the finite element model outputs are shown in Table 40. In order to compare the results between the line girder analysis and the finite element model output, the rating factors based on line girder analysis are presented in the bracket.

Table 37 – Refined Rating Factors of Floorbeam Using Finite Element Model

Limit State		Design Load		Legal Load			Legal Load
		Inv.	Op.	Type 3	Type 3-3	NJ 3S2	NJ-Permit
Strength I	Flexure	1.00 (0.63)	1.30 (0.81)	1.55 (1.35)	1.47 (1.63)	1.47 (1.34)	-
	Shear	3.47 (1.66)	4.50 (2.16)	5.31 (3.56)	6.18 (4.30)	5.44 (3.54)	-
Strength II	Flexure	-	-	-	-	-	0.91 (0.90)
	Shear	-	-	-	-	-	2.76 (2.39)
Service II		1.28 (0.80)	1.66 (1.04)	1.46 (1.27)	1.39 (1.54)	1.39 (1.26)	0.76 (0.75)

From the above table, it is easy to find the rating factors are markedly increased by using the finite element model. However, since the model was not calibrated by any testing, the results are not guaranteed and may lead to the unconservative ratings. As a result, the rating factors based on the finite element models are not adopted in this study due to the conservative concern. This model provides a basis that the FEM can be used for future study.

6.4. Legal Load Rating Using Site-Specific Live Load Factor

From Chapter 5, the site-specific live load factors for legal loads under Strength I limit state is determined by the mean value of the maximum live load factors from six (6) WIM sites, and the live load factors γ_L is calculated as 1.34. The generalized γ_L is 1.30 for ADTT ≤ 1000 per AASHTO MBE provisions. The bridge locates in the residential area and the truck volume is expected to be very low. According to the inspection report, the bridge had ADT of 404 in 2016, among which there is 1% truck traffic. The low ADTT should

theoretically reduce the live load factor. However, this site-specific live load factor does not incorporate with the ADTT, leading to the higher value of γ_L , indicating that the site may have a low volume of truck traffic but carry the heavier truck. The refined rating factors for each structural element are shown in Table 38 to Table 43. The values with strikethrough are the rating factors without using the site-specific live load factors. The actual member sizes are used for calculating the rating factors. In order to compare the results, the rating factors by using the generalized γ_L are shown in the bracket.

Table 38 – Refined Interior Stringer Rating Factors for Legal Loads

Strength I	Legal Load		
	Type 3	Type 3-3	NJ 3S2
Flexure	4.34 (4.48)	5.28 (5.45)	4.35 (4.49)
Shear	3.90 (4.03)	4.71 (4.87)	3.87 (4.00)

Table 39 – Refined Exterior Stringer Rating Factors for Legal Loads

Strength I	Legal Load		
	Type 3	Type 3-3	NJ 3S2
Flexure	4.82 (4.98)	5.87 (6.06)	6.00 (6.20)
Shear	5.51 (5.69)	6.66 (6.88)	6.80 (7.02)

Table 40 – Refined Floorbeam Rating Factors for Legal Loads

Strength I	Legal Load		
	Type 3	Type 3-3	NJ 3S2
Flexure	1.30 (1.34)	1.57 (1.62)	1.29 (1.33)
Shear	3.44 (3.56)	4.16 (4.30)	3.42 (3.53)

Table 41 – Refined Top Chord Rating Factors for Legal Loads

Strength I	Legal Load		
	Type 3	Type 3-3	NJ 3S2
Axial	1.84 (2.36)	1.46 (1.87)	1.35 (1.73)

Table 42 – Refined Bottom Chord Rating Factors for Legal Loads

Strength I	Legal Load		
	Type 3	Type 3-3	NJ 3S2
Axial	3.63 (4.72)	2.82 (3.66)	2.61 (3.40)

Table 43 – Refined Diagonal Rating Factors for Legal Loads

Strength I	Legal Load		
	Type 3	Type 3-3	NJ 3S2
Axial	4.17 (5.42)	3.34 (4.34)	3.08 (4.00)

Based on the above tables, although the live load factor is increased, all of the rating factors are all greater 1.0, indicating that there is no need to post the load limit.

Chapter VII

7. Conclusions

The analysis performed during the course of this research resulted in various different conclusion on the topic of load rating steel truss bridges with floorbeam system.

In the first stage of this research, a methodology for estimating the unknown structural member sizes of the bridge with no plans was investigated. Typically to load rate a bridge with no plans, the agencies hire engineering consultants to perform field investigations and obtain the required dimensions and size of components. However, it is both time consuming and costly to inspect every element of the structure. Taking advantage of the existing resources becomes important. The clustering methodology is proposed to load rate the steel truss bridges with no plans. The load rating procedure incorporates the information from the existing bridges that have plans with the field investigation of the bridges with no plans. By comparing the structural elements of the bridges with plans, clustering method could conservatively estimate the size of structural elements for bridges built during similar eras. The procedure would effectively reduce the amount of work needed for the field investigation for the agencies and would allow for the determination of the load carrying capacity. This study focuses on finding the correlation between these “similar” bridges and further validates the proposed load rating method. For each bridge that has no plans, similar bridges with known plans are screened from the bridge inventory and selected based on the bridge type, truss type, and year built. In the course of this study, to load rate a steel pony truss bridge without plans, six (6) similar bridges with plans were analyzed, and they

composed the bridge cluster to investigate the correlations between bridge geometries and the section sizes. This study indicates the following correlations:

- The stringer sizes are correlated with the stringer length and spacing. More geometric factors can be potentially involved, such as the slab thickness, but more bridges with plans are required to proceed the analysis.
- The floor beam sizes are correlated with the floorbeam length, the spacing, the number of the stringers, stringer length, and stringer spacing. In this study, only the floorbeam length and floorbeam are found to be directly strongly related to the member size. More correlations can potentially be proved in future study.
- The truss member sizes are influenced by the total loads resisted by the member, which is directly affected by the bridge width. The wider the bridge deck is, the bigger the truss member is. Also, the member length and bridge length are also found to have an impact on the truss member length.

This thesis aims at load rating a bridge with Structure No. 020033G which has no plans. Since most of the structural members on the steel bridges are exposed outside, the measurement would be very close to the as-built design sizes. In addition, the bridges with no plans are not on a large scale, so that the structural members, especially the girders and the truss members, are easy to access. Both the clustering method and the field inspection are performed for this bridge. According to the comparison between the clustering results and the field inspection results, the clustering method gives a good estimation of the member sizes as long as the bridge geometries are very similar. However, due to the limited number of bridges with plans, the clustering methodology could be more accurate if more similar bridges are incorporated in the cluster.

The second stage in this research focused on improving the accuracy of the rating factors. The rating factors obtained from the Stage I is based on the line girder analysis by incorporating AASHTO GDF equations. However, the live load effects of the floorbeam are found to be overly conservative. The finite element model was proposed to obtain live load effects. It is found that the finite element model provides much smaller live load effects on the floorbeam compared with line girder analysis so that the rating factors are improved accordingly. However, in this study, no live load testing has been performed, so that the model was not calibrated. It is proper to not use the live load effects from the uncalibrated model since it could potentially lead to the unconservative results. Although the live load model is used to assign the final rating factors, it still provides a basis to load rate a bridge by using the finite element model.

Besides the finite element model, the site-specific live load factors of legal truck for Strength I limit state are investigated in this study in order to improve the accuracy of the rating factors. The site-specific live load factor involves assessing the actual traffic data that pass through a specific site, addressing the live load uncertainties better than the generalized live load factor. On account of the low truck traffic volume on the target bridge and the big amount of the WIM systems in New Jersey, the site-specific live load factors for the legal load under Strength I limit state are investigated. By analyzing the WIM data from six (6) sites that locate at the same county as the bridge with no plans, the live load factors are taken as the mean of the maximum live load factor of each site, which is 1.58. This value is higher than the generalized live load factor for $ADTT \leq 1000$, which is 1.30, leading to the decrease of the load factors. While estimating the maximum live load effects

over a 5-year evaluation period, the tail end of the live load effect histogram was assumed to approach to both the Gumbel distribution and the Normal distribution.

REFERENCES

1. *AASHTO LRFD Bridge Design Specifications for Highway Bridges*, 7th ed. AASHTO, Washington, D.C., 2017.
2. American Association of State Highway and Transportation Officials (2018). *Manual for Bridge Evaluation*, 3rd ed. AASHTO, Washington, D.C.
3. Bridge Inspection Committee. (2013). Bridge Rating Manual. *Iowa Department of Transportation Office of Bridges and Structures*.
4. Bridge Inspection Committee. (2013). Bridge Inspection Program Manual. *Oregon Department of Transportation*.
5. Bridge Inspection Committee. (2014). Bridge Safety Inspection Policy and Procedure Manual. *Mississippi Department of Transportation Office of Bridges and Structures*.
6. Bridge Inspection Committee. (2017). Bridge Load Rating Guidelines. *State Of Rhode Island Department of Transportation*.
7. Bridge Inspection Committee. (2018). Bridge Inspection Manual. *Texas Department of Transportation Administrative and Engineering Publications*.
8. Bridge Inspection Committee. (2018). Washington State Bridge Inspection Manual. *Washington: Washington State Department of Transportation Administrative and Engineering Publications*.
9. Ghosn, M., Sivakumar, B., and Miao, F. (2011). *Load and Resistance Factor Rating (LRFR) in NYS*, vol. I and II. Final report, Department of Civil Engineering, The City College of The City University of New York, Project No. C-06-13.
10. Moses, F. (2001). *Calibration of Load Factors for LRFR Bridge Evaluation*. National Cooperative Highway Research Program (NCHRP). Transportation Res. Board NCHRP Rep. No. 454.
11. Mlynarski, M., Wassef, W.G., and Nowak, A.S. (2011). *A Comparison of AASHTO Bridge Load Rating Methods*. National Cooperative Highway Research Program (NCHRP). Transportation Res. Board NCHRP Rep. No. 700.
12. *NJDOT Design Manual for Bridge & Structures*, 6th ed. NJDOT, Trenton, 2016.
13. Nowak, A.S. (1999). *Calibration of LRFD Bridge Design Code*. National Cooperative Highway Research Program (NCHRP). Transportation Res. Board NCHRP Rep. No. 368.
14. Rooper. (2013). Methods Used to Obtain Measurements of a Large Truss Bridge with No Plans. *Oregon Department of Transportation* (Conference presentation).

15. Sivakumar, B., Ghosn, M., Moses, F., and TranSystem Corporation (2011). *Protocols for Collecting and Using Traffic Data in Bridge Design*. National Cooperative Highway Research Program (NCHRP). Transportation Res. Board NCHRP Rep. No. 683.
16. Sivakumar, B., Moses, F., Fu, G., and Ghosn, M. (2007). *Legal Truck Loads and AASHTO Legal Loads for Posting*. National Cooperative Highway Research Program (NCHRP). Transportation Res. Board NCHRP Rep. No. 575.
17. Uddin, N., Zhao, H., Waldron, C., Dong, L., and Greer, S. (2011). *Weigh-in-Motion (WIM) Data for Site-Specific LRFR Bridge Load Rating*. Report to Alabama DOT, Department of Civil, Construction, and Environmental Engineering University of Alabama at Birmingham.